PAGEOPH, Vol. 124, Nos. 1/2 (1986)

0033-4553/86/020225-44$1.50+0.20/0

Fluid Infiltration into Fault Zones: Chemical, Isotopic, and Mechanical Effects

R. KERRICH[1]

Abstract—Fluid infiltration into fault zones and their deeper-level counterparts, brittle–ductile shear zones, is examined in diverse tectonic environments. In the 2.7 Ga Abitibi greenstone belt, major tectonic discontinuities, with lateral extents of hundreds of kilometres initiated as listric normal faults accommodating rift extension and acted as sites for komatiite extrusion and locally intense metasomatism. During reverse motion on the structures, accommodating shortening of the belt, these transcrustal faults were utilised as a conduit for the ascent of trondhjemitic magmas from the base of the crust and of alkaline magmas from the asthenosphere and for the discharge of thousands of cubic kilometres of hydrothermal fluids. Such fluids were characterised by $\delta^{18}O = +6 \pm 2$, $\delta D = -50 \pm 20$, $\delta^{13}C = -4 \pm 4$, and temperatures of 270 to 450 °C, probably derived from devolatilisation of crustal rocks undergoing prograde metamorphism. Hydrothermal fluids were more radiogenic ($^{87}Sr/^{86}Sr = 0.7010$ to 0.7040) and possessed higher μ than did contemporaneous mantle, komatiites or tholeiites, and thus carried a contribution from older sialic basement. A provinciality of $^{87}Sr/^{86}Sr$ and $\delta^{13}C$ is evident, signifying that fault plumbing sampled lower crust which was heterogeneous at the scale of tens of kilometres. Mineralised faults possess enrichments of large ion lithophile (LIL), LIL elements, including K, Rb, Ba, Cs, B, and CO_2, and rare elements, such as Au, Ag, As, Sb, Se, Te, Bi, and W. Fluids were characterised by $X_{CO_2} \approx 0.1$, neutral to slightly acidic pH, low salinity $\leqslant 3$ wt-%, K/Na = 0.1, they carried minor CH_4, CO, and N_2, and they underwent transient effervescence of CO_2 during decompression. Clastic sediments occupy graben developed at fault flexures. The $^{40}Ar/^{39}Ar$ release spectra indicate that fault rocks experienced episodic disturbance on time scales of hundreds of millions of years.

At the Grenville front, translation was accommodated along two mylonite zones and an intervening boundary fault. The high-temperature (580 °C) and low-temperature (430 to 490 °C) mylonite zones, formed in the presence of deep-level crust-equilibrated fluids of metamorphic origin. Late brittle faults contain quartz veins precipitated from fluids with extemely negative $\delta^{18}O$ (−14 per mil) at 200 to 300 °C. The water may have been derived from downward penetration into fault zones of precipitation of low ^{18}O on a mountain range induced by continental collision, with uplift accommodated at deep levels by the mylonite zones coupled with rebound on the boundary faults.

Archean gneisses overlie Proterozoic sediments along thrust surfaces at Lagoa Real, Brazil; the gneisses are transected by brittle–ductile shear zones locally occupied by uranium deposits. Following deformation at 500 to 540 °C, in the presence of metamorphic fluids and under conditions of low water-to-rock ratio, shear zones underwent local intense oxidation and desilication. All minerals undergo a shift of −10 per mil, indicating discharge of meteoric-water-recharged formation brines in the underlying Proterozoic sediments up through the Archean gneisses, during overthrusting; ≈ 1000 km^3 of solutions passed through these structures. The shear zones and Proterozoic sediments are less radiogenic ($^{87}Sr/^{86}Sr = 0.720$) than contemporaneous Archean gneisses (0.900), corroborating the transport of fluids and solutes through the structure from a large external reservoir.

Major crustal detachment faults of Tertiary age in the Picacho Cordilleran metamorphic core complex of Arizona show an upward transition from undeformed granitic basement through mylonitic to

[1] Department of Geology, University of Western Ontario, London, Ontario, Canada N6A 5B7.

brecciated and hydrothermally altered counterparts. The highest tectonic levels are allochthonous, oxidatively altered Miocene volcanics. This transition is accompanied by an increase of 12 per mil in $\delta^{18}O$, from +7 to +19, and a 400 °C decrease in temperature. Lower tectonic levels acted as aquifers for the expulsion of large volumes of higher-temperature reduced metamorphic fluids and/or evolved formation brines. The Miocene allochthon was influenced by a lower-temperature reservoir inducing oxidative potassic alteration; mixing occurred between cool downward-penetrating thermal waters and the hot, deeper aqueous reservoir.

In general, flow regimes in these fault and shear zones follow a sequence, from conditions of high temperature and pressure with locally derived fluids at low water-to-rock ratios, during initiation of the structures, to high fluxes of reduced formation or metamorphic fluids along conduits as the structures propagate and intersect hydrothermal reservoirs. Later in the tectonic evolution and at shallower crustal levels there was incursion of oxidising fluids from near-surface reservoirs into the faults. In general, magmatism, tectonics, and fluid motion are intimately related.

Key words: Fluid infiltration, geochemical transport, faults, isotopes, hydraulic fracturing.

1. Introduction

Fluid penetration through major structures—specifically faults, thrusts, and their deeper-level extensions, brittle–ductile shear zones—is a phenomenon well-established both by contemporary observations of seismic pumping (SIBSON et al., 1975; SIBSON, 1981, 1982) and by evidence of hydration or extensive hydrothermal metasomatism in ancient counterparts. On a global scale faults play a key role in the geochemical cycle, where volatiles from the hydrosphere are transferred to rocks as hydroxyl and carbonate minerals, subsequently being returned to the surface by release along faults during burial, compaction, and devolatilisation accompanying metamorphism. It has been pointed out, for instance, that faults at continental margins may act as one of the sites for return flow of the $\approx \times 1.5$ to 3×10^{21} gm of H_2O per Ma, released during the subduction of hydrated oceanic lithosphere (FYFE and KERRICH, 1985; WANG, 1980).

The mechanical and chemical roles of fluids in fault and shear zones have been examined by a number of authors for eroded remnants of structures (BEACH and FYFE, 1972; BEACH, 1976; KERRICH et al., 1977, 1980, 1984; FYFE et al., 1978; ETHERIDGE and COOPER, 1981; FYFE and KERRICH, 1983, 1985) and for their seismically active modern counterparts (IRWIN and BARNES, 1975; SIBSON, 1982); there is, however, little quantitative information on the origin of the fluid reservoirs implicated, the chemical mass transport involved, the ambient temperature and pressure, physical and chemical properties, hydraulic conditions, or possible evolution of fluid regimes through a history of progressive incremental displacement along the structures.

This paper sets out to examine the variety of fluid regimes in fault zones, utilising information from structures in four areas, which encompass a variety of tectonic

environments, styles of deformation, lithological groups, and ages. These are as follows.

1. Fault systems of the Abitibi greenstone belt ($\approx$ 2700 Ma).
2. Structures at the Grenville front ($\approx$ 1100 Ma).
3. Shear zones aged $\approx$ 820 Ma in Archean gneisses at Lagoa Real, Brazil.
4. Detachment faults in Cordilleran metamorphic core complexes, of Tertiary age.

The selection of these structural domains was based on existing mapping and documentation of the faults as major structural features tens to hundreds of kilometres in lateral extent. In addition, the presence of sporadically developed mineralisation provides the opportunity to evaluate fluid regimes associated with the faults.

Specific questions to be considered in the context of fluid transport through faults are the following.

1. Geochemical transport accompanying deformation and/or fluid infiltration.
2. Sources of volatile components, such as H_2O, CO_2, and H_2S.
3. The nature of rock reservoirs donating lithophile and other elements locally enriched in faults.
4. Ambient temperature–pressure and hydraulic conditions.
5. The history of incremental displacement and fluid activity.
6. The presence of highly sodic or alkaline magmas along some structural lineaments.

This paper draws on earlier articles concerning 'fluid participation in deep fault zones' (KERRICH et al., 1984; KERRICH, 1985), reports new data for previously described regions, and extends coverage of the subject with reference to additional tectonic situations. Faults almost invariably have poor surface exposure. In view of this, materials, for the study were obtained mostly from mines and their environs which were located on or near fault structures and thus afforded access to unweathered materials in open pits or underground.

2. *Abitibi greenstone belt faults*

2.1 Geological setting

The 2.7 Ga Abitibi greenstone belt, located in the Superior Province, is composed of an array of volcanic-plutonic complexes with intervening belts of volcaniclastic,

clastic, and chemical sedimentary rocks (GOODWIN and RIDLER, 1970). Prehnite-pumpellyite to lower greenschist facies of regional or hydrothermal metamorphism predominates, except in the periphery of batholiths, where amphibolite facies rocks may be present (JOLLY, 1978).

A prominent feature of the greenstone belt is a series of major east-west-trending tectonic discontinuities or fault zones, locally termed 'breaks', which extend for hundreds of kilometres (Fig. 1, a, b). Two of the dominant structures are the east-west-trending Destor-Porcupine and Kirkland-Lake–Cadillac-Bouzan fault zones; in the Kirkland Lake area these structures mark the north and south limbs of a regional east-plunging synclinorium; see Figure 1b (THOMSON, 1941; JENSEN, 1976; JENSEN and LANGFORD, 1983). The magnitude and direction of translation on these structures are not well quantified. The structures control the linear disposition of ultramafic rocks and locally delimit linear belts of clastic or chemical sedimentary rocks. The structures also acted as preferential sites for the emplacement of trondhjemitic and alkaline magmas and were locally domains of intense hydrothermal metasomatism, exemplified by rich lode gold deposits.

2.2 Metasomatism in fault zones: Calculations of chemical mass balance

Quantitative evaluation of chemical mass transport in metasomatised fault zones requires knowledge of the composition of rocks in the original and altered states together with the constraints on any possible volume changes. GRESENS (1967) suggested incorporating specific-gravity data into two-way mass-balance calculations, such that fixing either volume change or the behaviour of one component during a reaction provides a unique solution. For any metasomatic transformation of parent rock to altered product, volume factors f_v may be computed which correspond to the isochemical behaviour of individual components. Clustering of the volume factors of several components that are empirically known to be relatively immobile (such as TiO_2, Al_2O_3, Sc, Hf, and Zr) then provides a rational basis for estimating the volume change of the reaction as a whole. In the notation used by GRESENS (1967), $f_v = 1$ signifies constant-volume metasomatic alteration of reactants to products; $f_v = 0.8$ and $f_v = 2.0$, for example, correspond to 20 vol-% reduction and 100 vol-% increase, respectively. Furthermore, rigorous calculations of chemical mass balance require that the series of altered rocks, along with the unaltered precursor, belonged to an initially chemically uniform population. It is important to emphasise that the observed metasomatically altered products represent specified finite changes relative to the precursor, but that such changes may have been arrived at via a complex sequence of incremental chemical transfers.

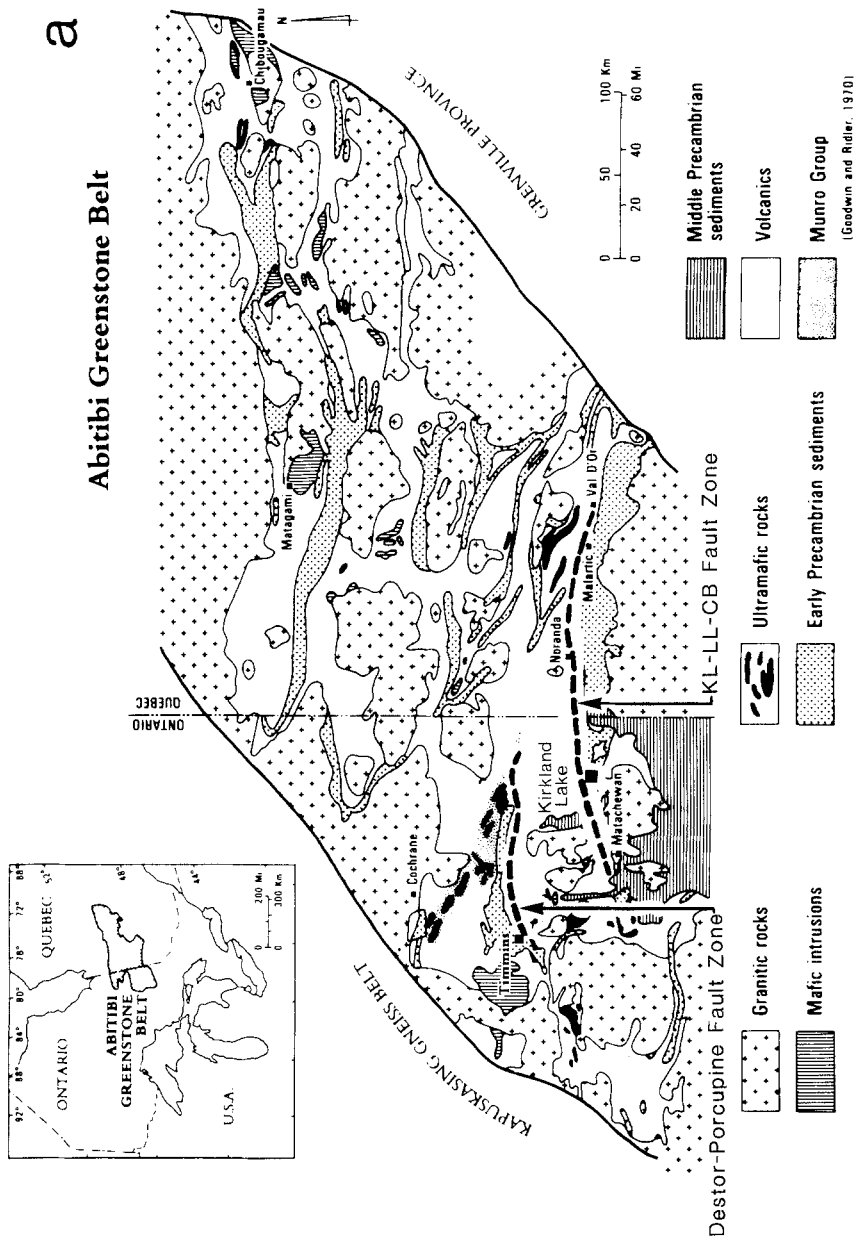
a
Abitibi Greenstone Belt
Chibougamau
Matagami
Val D'Or
Malartic
Noranda
Kirkland Lake
Malachewan
Cochrane
Timmins
KL-LL-CB Fault Zone
Destor-Porcupine Fault Zone
KAPUSKASING GNEISS BELT
GRENVILLE PROVINCE
ONTARIO
QUEBEC
0 20 40 60 Mi
0 50 100 Km
Middle Precambrian sediments
Volcanics
Munro Group
(Goodwin and Ridler, 1970)
Ultramafic rocks
Early Precambrian sediments
Granitic rocks
Mafic intrusions
QUEBEC
ONTARIO
U.S.A.
ABITIBI GREENSTONE BELT
0 200 Mi
0 300 Km

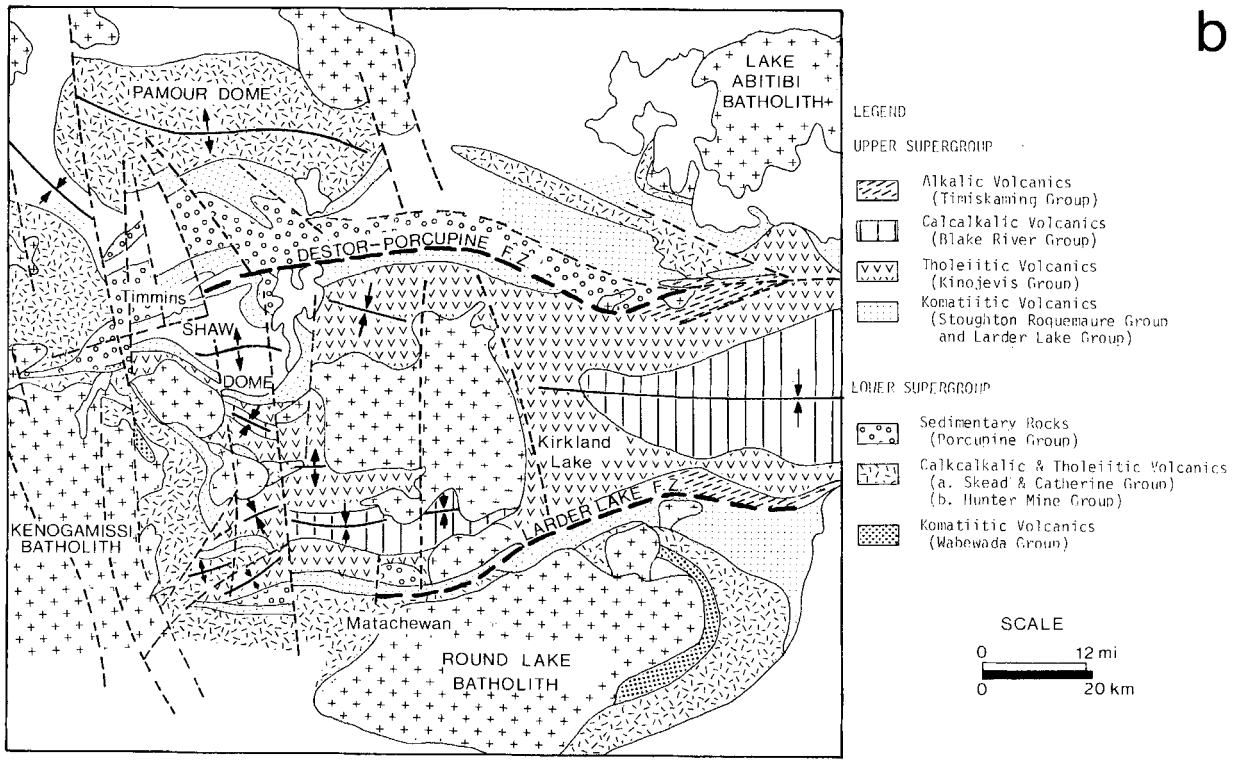

Figure 1
(A) Schematic geology of the Abitibi belt. After GOODWIN and RIDLER, 1970. KL-LL-LB refers to the Kirkland Lake–Larder Lake—Cadillac-Bouzan fault zone. (B) Geology of the Kirkland Lake area. After JENSEN, 1978 a, b; 1980.

2.3 *Hollinger Fault, Timmins: Patterns of alteration*

Major structures in the Timmins district display at least three episodes of translation, which are associated with (a) magmatism, (b) fluid transport, and (c) sedimentation, respectively. Early extensional displacements on listric faults are associated with komatiitic flows and clastic sediments; spilitisation of the volcanics in the presence of marine water occurs at this stage, and may lead to coeval chemical sediments at volcanic centres or along faults, or both. Reverse motion is associated with trondhjemitic magmatism and major fluid discharge linked to gold deposits. At late stages during wrench faulting, domains of relaxation are the sites of molasse sedimentation in graben and alkalic magmatism, and also of the infiltration of meteoric waters. In this section we are concerned with the second 'main stage' of fluid discharge.

Intense metasomatic alteration along faults and their bounding wall rocks is marked by massive fixation of a select group of lithophile elements or components, including Si, CO_2, K, Rb, Ba, Cs, B. Such additions are reflected in the presence of veins typically composed of quartz, ferroan dolomite, muscovite, and sulphide minerals, collectively bounded by altered wall rocks. Numerous generations of veins, variably modified by intracrystalline deformation, attest to repeated cycles of volatile fluxing with intervening episodes of incremental ductile deformation (cf. KERRICH and ALLISON, 1978; KERRICH, 1983; KISHIDA, 1984). The magnitude of volatile flux through the structures, with its associated lithophile element fixation, is illustrated by the estimate that, for the known length of fault zones, about 8,000 km^3 of aqueous fluids were discharged along the faults, precipitating in the process 60×10^{15} gm of Si, 30×10^{15} gm of CO_2, and 6×10^{15} gm of K (KERRICH et al., 1986, in press).

The Hollinger fault, a splay of the Porcupine-Destor fault system, traverses a variety of different rock types where it outcrops in open pits at the surface. This fault is representative of the greenstone belt structures under consideration here, in respect of the variety of lithologies present, the tectonic style, and the range of metasomatic phenomena. Despite the combined effects of deformation and metasomatic alteration, host rocks of original trondhjemitic, basaltic, and ultramafic parentage can be identified on the basis of the ratios of the less mobile major and trace elements (KERRICH, 1983). Chemical transfers in the rocks of probable ultramafic origin are plotted in Figure 2, to illustrate the nature and magnitude of fault-related metasomatism.

Given that no perfectly fresh rocks are present, calculations of chemical mass balance have been conducted by matching the diagnostic 'immobile element' ratios of the three populations given above to analyses of fresh rocks from the Timmins area. An average of the analyses for three komatiite flows from Munro township (NESBITT and SUN, 1976, Table 1, 8–11) is utilised here as a hypothetical parental rock, based on compliance of Ti/Zr, Zr/Y, Al_2O_3/TiO_2, and Ni between this population of fresh rocks and the Hollinger altered counterparts. Considering the values of the above interelement ratios, coupled with the positive correlation of MgO to Ni

and an inverse relationship of MgO to TiO_2 in fresh komatiites, the Hollinger ultramafic rocks probably had primary MgO contents in the range of 22 to 26 wt-%.

It is not possible with the present sampling to establish the extent of chemical modification of the ultramafic rocks arising from possible hydrothermal alteration shortly after extrusion, or the chemical effects of deformation prior to later hydrothermal alteration associated with the auriferous quartz-carbonate veins. Enhanced $\delta^{18}O$ values for silicate minerals likely signify isotopic exchange with marine, or evolved marine water at temperatures of $<200\,^{\circ}C$ ($\delta^{18}O$ for chlorite, $+16$ per mil).

Carbonate minerals, interlaminated with ultramafic tuff and of possible sedimentary origin, are cloudy, fine-grained, anhedral, and in the compositional range of high-magnesium dolomite, with no significant Mn substitution (KERRICH, 1983, Fig. 22). Where recrystallised at vein margins, the carbonates are compositionally ferroandolomite. Secondary carbonates texturally associated with quartz-chlorite-muscovite-gold veins in faults are clear, coarse-grained, anhedral, and within the magnesite-siderite solid-solution series. Overall, the ultramafic rocks have undergone a massive loss of iron, compared to their precursors; the observed trend of iron enrichment in secondary carbonates could partly be accounted for by transfer of iron from a silicate reservoir to a carbonate reservoir accompanying the hydrolysis of chlorite to muscovite in vein wall rocks. Both vein-related muscovite and chlorite contain $\approx 1\%$ Cr_2O_3, reflecting the elevated chromium content of the ultramafic host rock.

The geochemical results for altered ultramafic rocks at Hollinger form two data arrays: a low K_2O series and a high one; see Figure 2. The former are remote from fault-hosted veins, have been leached to low volume factors (0.8 to 0.9), reflecting the extensive volumetric contraction accompanying the removal of major-element oxides, and possess low K_2O, Au, Rb, Ba, As, and Sb, whereas the latter group are adjacent to veins in faults and are characterised by massive additions of these elements. Taking the geological, textural, mineral, chemical, isotopic, and geochemical lines of evidence collectively, it is suggested that the ultramafic rocks at Hollinger underwent an early stage of seawater and/or metamorphic fluid-induced alteration under conditions of low T and P_{CO_2} in the submarine environment. This stage involved loss of Si, Fe, Mn, Mg, Na, and K, with gains of Sr plus volatiles, reflected in early laminated carbonates, during hydrolysis of primary silicate minerals to zeolites and clays. Subsequently, at deeper crustal levels under ambient conditions of higher T and P_{CO_2} during vein emplacement, the rocks experienced massive gains of CO_2, K, Rb, and Ba, and minor fixation of Fe, Ca, and Mn, as represented by the conversion of clays and zeolites, or their greenschist facies products, to secondary iron, magnesium-carbonates, muscovite, and chlorite (Fig. 2). Additional sodium may have been lost during hydrothermal alteration associated with vein emplacement, giving the low observed content of Na_2O.

Patterns of rare-earth elements for the series of low and high K_2O rocks, respectively have flat configurations characteristic of most Archean komatiites, but the

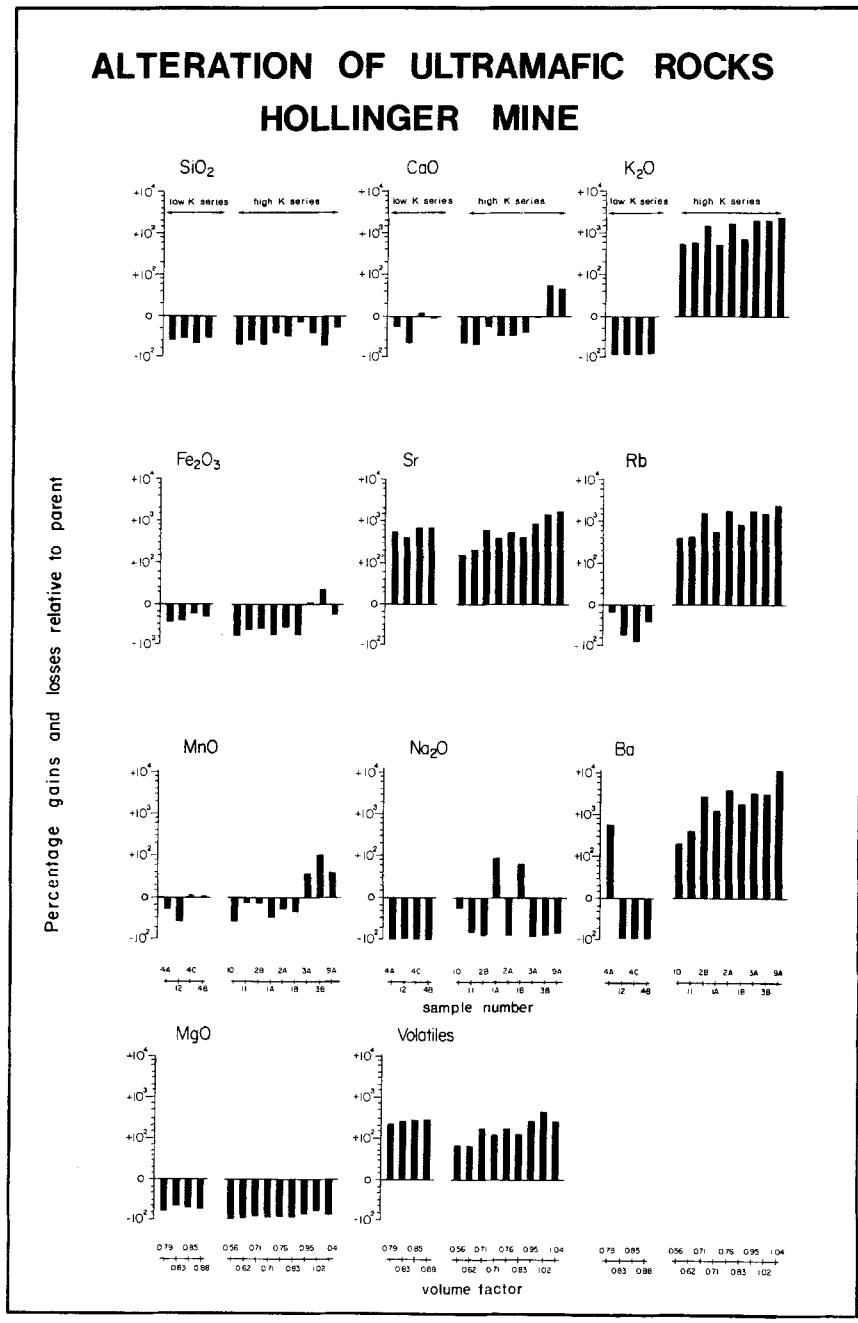

Figure 2

Gains or losses of major-element oxides and selected trace elements hydrothermally altered in rocks of primary ultramafic compositions (peridotitic komatiites), Hollinger Mine, number 12 vein, open pit. Gains and losses expressed as percentage changes relative to abundances in unaltered parent rock, and ordered according to increasing volume factor. After KERRICH, 1983.

high-K_2O mineralised rocks have systematically larger abundances by a factor of 1.5 to 2; see Figure 3, a, b). This cannot be fully accounted for by enrichment during volumetric contraction and therefore signifies either some absolute enrichment of the rare earth elements accompanying hydrothermal alteration (see also KERRICH and FRYER, 1979, LUDDEN, et al., 1984) or, alternatively, primary differences in the absolute abundances of rare-earth elements between neighbouring komatiitic units. Under low-temperature hydrothermal conditions the REE are relatively insoluble and accordingly behave isochemically. If appropriate ligands such as F or CO_3^{2-} are present, significant aqueous transport of the rare-earth elements is possible; such effects have been reported by KERRICH and FRYER (1979).

Many rocks have experienced volume losses of 20% during the successive episodes of hydrothermal alteration, with absolute cumulative depletions of SiO_2, Fe_2O_3, CaO, MgO, and Na_2O in excess of the total gains of volatiles and K_2O. Given the conservative behaviour of aluminium, these overall losses of chemical components have left the rocks relatively aluminious, and such hydrothermal leaching may promote flow focus within fault zones.

Fluids which induced the K–Si–CO_2 alteration in proximity to veins, and from which the auriferous veins were precipitated, were at temperatures of ≈ 400 °C, with fluid $\delta^{18}O$ of 7 ± 1 per mil, and at low redox potential; the latter property is indicated by the absence of Fe^{3+} silicates or oxides in the alteration mineral assemblage. Studies of primary liquid inclusions in vein quartz show filling temperatures of 360 °C (filling temperatures are a minimum estimate of the real temperature of hydrothermal mineral growth) and salinities of < 1.5 wt-% NaCl equivalent, and reveal the presence of significant liquid CO_2. Pressures are estimated at 2 to 3 kbar.

2.4 Source of volatile components in fault zones

The source, temperature, and magnitude of aqueous fluid reservoirs participating in major fault zones of the Abitibi greenstone belt have been evaluated from oxygen and hydrogen isotope data. Five distinct terrestrial fluid reservoirs have been identified on the basis of their oxygen and hydrogen isotope compositional ranges. These are marine, meteoric, magmatic, and metamorphic fluids, together with formation brines that generally contain a large component of 'evolved' meteoric recharge waters (TAYLOR, 1974); see Figure 4A. Oxygen isotope studies also permit estimates of ambient mineral and fluid temperatures at equilibrium, given that the fractionation of oxygen isotopes between coexisting silicates or metal oxides is a function of temperature alone (JAVOY, 1977; FRIEDMAN and O'NEIL, 1977). The problems of identifying fluid flow through rocks are particularly amenable to evaluation by oxygen isotope analyses, since isotopic exchange between rocks and an aqueous reservoir is reflected in shifts of $\delta^{18}O$ rock or mineral from an initial value by a magnitude that depends on the $\delta^{18}O$ fluid, ambient temperature, the fluid-to-rock ratio, and the extent of approach to equilibrium (TAYLOR, 1974, 1979).

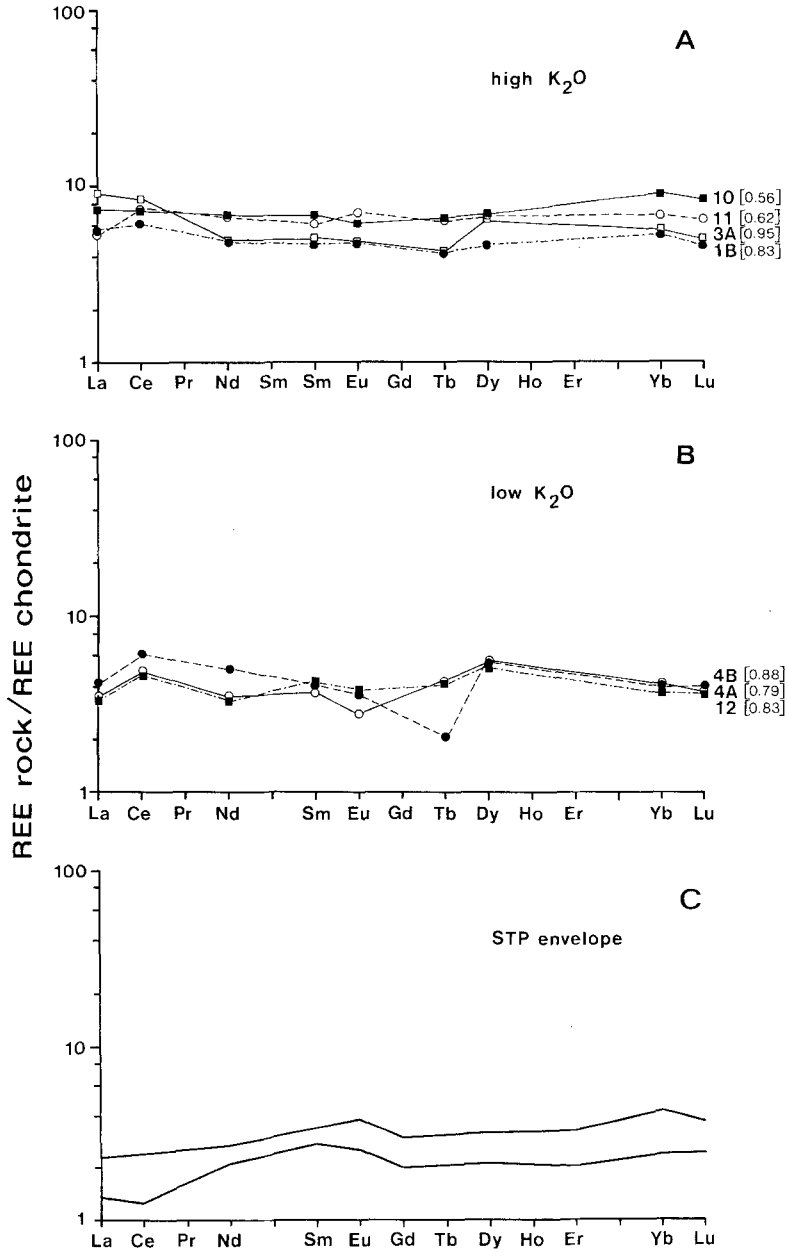

Figure 3

(A) Chondrite normalised rare-earth-element distributions for mineralised rocks of original ultramafic composition, number 12 vein, Hollinger Mine. Bold figures are sample numbers; figures in square brackets are deduced volume factors of alteration. (B) Rare-earth-element patterns for unmineralised counterparts, contiguous with those in A above. (C) Rare-earth-element envelope for relatively fresh komatiites (formerly termed 'peridotitic komatiites' and sometimes termed 'STP' for 'spinifex textured peridotites' (cf. NESBITT and SUN, 1976).

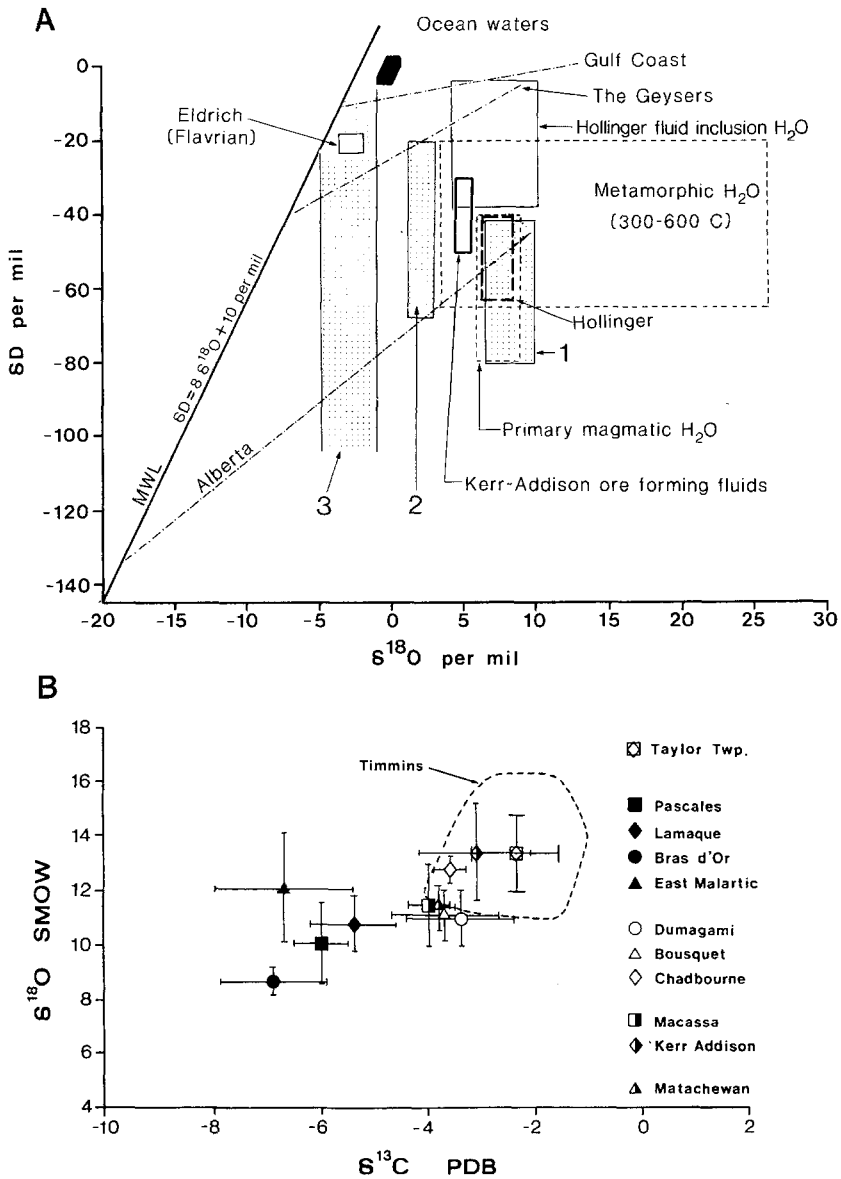

Figure 4

(A) Isotopic composition of natural terrestrial fluid reservoirs in δD versus $\delta^{18}O$ coordinate space. After TAYLOR, 1974. Superimposed are calculated fields for three vein stages at Macassa, one ore solution, two fluids associated with selenite deposition in faults, three late-stage quartz-magnetite stringers; after KERRICH and WATSON, 1984. Hollinger data from work reported, this paper; Kerr Addison data from KISHIDA and KERRICH, 1986; and Eldrich data from KENNEDY, 1985. Data for H_2O decrepitated from quartz veins of the Hollinger mine are from FYON et al., 1984. (B) Fields of different carbonates plotted on $\delta^{13}C$ versus $\delta^{18}O$ coördinate space; field for Timmins is after FYON et al., 1984.

A compilation of oxygen isotope data for hydrothermal silicates from mineralised fault zones is given in Table 1, and calculated fluid isotopic compositions are summarised in Figure 4A. A significant feature of the mineral results is that the $\delta^{18}O$ of hydrothermal quartz, muscovite, and chlorite lie within narrow intervals, signifying uniform hydrothermal conditions. For instance, at the Dome Mine, Timmins, located close to the Porcupine-Destor fault, all of the vein quartz from five different mineralised domains have a restricted range of $\delta^{18}O$ of 14 to 15.2; Δ quartz-muscovite and Δ quartz-chlorite are relatively constant at 3.5 to 4.0 and at 5.5 to 6.1 per mil respectively, corresponding to calculated isotopic temperatures of 270 to 450 °C and a fluid isotopic composition of 7 ± 1 per mil ($1\ \sigma$).

Considering the data for fourteen fault-hosted mineral deposits collectively distributed over distances of several hundred kilometres along the two main fault systems, the overall estimated range of ambient fluid temperatures is 270 to 450 °C, with a fluid isotopic composition given by $\delta^{18}O = 6 \pm 2$ per mil and $\delta D = -50 \pm 20$ per mil; see Figure 4A. The calculated fluid compositions are consistent with the range of most fluids implicated in metamorphism and overlap the magmatic field; see Figure 4A (cf. TAYLOR, 1974). Marine or meteoric waters may undergo isotopic evolution from primary signatures towards δD and $\delta^{18}O$ values regarded as characteristic of magmatic fluids, during high-temperature isotopic exchange with crustal rocks under conditions of low water-to-rock ratio. Fluids that have followed such an exchange trend, however, also tend to become saline, whereas the fluids implicated in fault metasomatism were of low salinity (see below). Accordingly, participation of evolved marine or meteoric waters at this stage of fault-related fluid activity and metasomatism probably may be ruled out. The inferred metamorphic fluids, with a possible magmatic component, are considered to be generated during progressive accumulation and burial of the volcanic-sedimentary sequences and, hence, broadly contemporaneous with volcanic-plutonic-tectonic activity.

The observed narrow interval of 11 to 15 per mil for $\delta^{18}O$ in vein quartz is independent of wall-rock lithology. Quartz in wall rocks is shifted from initial values towards that of vein quartz in proximity to zones of intense metasomatism. These relations signify both an approach to isotopic equilibrium and fluid-dominated conditions along fault structures. A corollary of these results is that lateral diffusion of such chemical components as CO_2, K, and Au from wall rocks into fault zones (cf. BOYLE, 1961, 1979) is incommensurate with the isotopic data.

The ubiquitous presence of hydrothermal carbonates, along with quartz, in mineralised fault zones provides evidence that the fluid reservoir carried significant CO_2, raising the question of the source of the carbon. The oxygen and carbon isotope compositions of hydrothermal carbonates, principally from fault-hosted lode gold deposits, are summarized in Figure 4B. For the majority of data, carbonates occupy a restricted field, where $\delta^{18}O$ spans 10 to 17, and $\delta^{13}C$ -8 to -0.5, per mil.

In general, quartz-carbonate pairs are out of oxygen isotope equilibrium,

Table 1

*Oxygen Isotope Composition of Minerals Separated from Gold-bearing Veins and their Host Rocks in Mines from the Yellowknife Timmins, and Val d'Or Districts, together with Calculated Isotopic Temperatures and $\delta^{18}O$ Fluid**

		$\delta^{18}O$ vein quartz	$\delta^{18}O$ mineral	$\delta^{18}O$ host quartz	Δ quartz-mineral	Temp. (°C)	$\delta^{18}O$ fluid
Yellowknife District, Campbell shear	Gold-bearing quartz-carbonate veins, 2300 in sericite-chlorite schist	12.48		12.06			
		12.53	6.58 c		5.95	440	8.2
		11.50	5.97 c		5.53	480	7.9
		11.59	7.03 m		4.56	320	7.5
	4900	11.43		11.29			
	5100	10.80					
Con shear	Gold-bearing quartz-carbonate veins, 250	12.25					
		11.50	5.97 c		5.53	480	7.9
	in sericite-chlorite schist 1550	12.06		12.13			
Giant shear, east zone H.G. zone open pit	Gold-bearing quartz-carbonate veins in sericite-chlorite schist	12.28					
		12.77		12.57			
		12.01					
Western granodiorite	Gold-bearing quartz veins emplaced into shear zone within graniorite	13.03		13.70			
Ptarmigan	Gold-gearing quartz veins in metagreywacke	12.60	6.67 c		5.93	440	8.2
		13.16		13.91			
Surface	Gold-bearing quartz-carbonate veins in metabasalts	13.51	6.70 c		6.81	370	7.6
		13.56	7.45 c		6.11	420	8.9
Dome Mine, Timmins	Banded quartz-muscovite veins in ultramafic schist	14.74	10.98 m		3.76		
		14.41	11.28 m	14.66	3.13		
		14.37	10.78 m		3.59	430	9.8
		14.52	10.54 m		3.98	380	8.8
		14.63		15.17			
	Banded quartz-tourmaline veins	15.07					
		15.24					
	Veins in quartz-feldspar porphyry	14.97		15.31			
		13.93		13.87			
		14.19	8.05 c	14.26	6.14	420	9.6
	Quartz-tourmaline veins in dacite	15.09	9.21 c		5.88	440	10.8
		15.17	9.38 c		5.79	450	11.1
	Quartz veins in Timiskaming slates	14.65		14.10			
		14.52		15.77			
		14.76	11.26 m		3.50	440	10.5
	Quartz-carbonate veins in metabasic schists	14.53	8.99 c	14.84	5.54	480	10.9
		15.20					
	Quartz-carbonate veins parallel to auriferous stratiform carbonate	14.87	9.31 c	15.32	5.56	480	11.6

Table 1 *continued*

		$\delta^{18}O$ vein quartz	$\delta^{18}O$ mineral	$\delta^{18}O$ host quartz	Δ quartz-mineral	Temp. (°C)	$\delta^{18}O$ fluid
Aumor Mine, Timmins	Quartz veins parallel to auriferous stratiform carbonate	14.65 15.01					
MacIntyre Mine	Quartz-carbonate veins 1526 stope	15.02 14.96	10.62 m	14.86	4.40	340	8.2
	Quartz-carbonate veins, 4675-5 vein	14.81 14.74	10.80 m	14.90	4.01	380	9.2
Paymaster	Quartz-carbonate-chlorite veins; mine dump	14.87 14.89	9.17 c		5.70	460	10.9
	Silicified Au-bearing porphyry	14.80 14.62					
Hollinger	Quartz-carbonate veins in altered ultramafic tuffs	13.5	7.7		5.8	440	9.1
Chadbourne	Quartz-albite-carbonate veins in fractured basalt and andesite	12.0 to 13.5	6.1 to 6.9		5.9 6.8	380 to 450	8.1
			8.1 to 8.9		3.6 to 4.0		
Kerr Addison Mine	Quartz-muscovite-carbonate veins in carbonate sediment	14.48	10.54 m		3.94	390	9.0
	'Flow ore,' albitic-pyrite tuffs and flows	14.4	12.0 ab 6.9 c		4.2	350	8
	'Flow ore', muscovite pyrite tuffs and flows	14.2	10.1 m				
Lamaque	Quartz-tourmaline-carbonate veins Main granodiorite	12.84 12.71 12.79	6.54		6.30	410	7.8
Pascales	Quartz-tourmaline-carbonate veins	11.86 11.58	5.71 c		6.15	420	8.1
Bras d'Or	Quartz-tourmaline-carbonate veins	11.61 12.70	5.61 c		6.00	430	8.2
East Malartic	Albite-orthoclase-quartz-tuffaceous chert	13.4 to 21.7	10.4 to 12.3 (ab)			200	0.1
			14.1 to 16.7 (or)			150	0.1

* Abbreviations: c, chlorite; m, muscovite; ab, albite; or, orthoclase. Isotopic temperatures and fluid $\delta^{18}O$ calculated from the mineral-water fractionation equations reported by CLAYTON et al., (1972) for quartz, O'NEIL and TAYLOR (1967) for feldspars, O'NEIL *et al.* (1969) for muscovite, and WENNER and TAYLOR (1971) for chlorite.

probably because of the susceptibility of carbonates to retrograde oxygen exchange. The carbon isotope compositions define a narrow field, compared to most other hydrothermal systems.

Carbon of -8 to -0.5 per mil could be derived from a number of different carbon reservoirs, given that the average $\delta^{13}C$ of igneous, sedimentary, and metamorphic rocks is about -5 and that of juvenile carbon is -5 ± 2 (OHMOTO and RYE, 1979). KERRICH (1983) and GOLDING and WILSON (1983) have argued on the basis of carbon isotope data and geological considerations that the hydrothermal CO_2 in Archean structurally hosted gold deposits is derived from a mixture of juvenile carbon and marine carbonate with variable proportions of reduced carbon. FYON et al. (1984) propose a mantle origin for the CO_2. A contribution of carbon from the oxidation or hydrolysis of hydrocarbons low in ^{13}C in interflow sediments at source is likely and would account for the most depleted values (Fig. 4B).

A key feature is the provinciality of $\delta^{13}C$ carbonate values (Fig. 4B). Redox-dependent fractionations accompanying the precipitation of carbonates account for, at most, a shift of $+2$ per mil, and some of the most depleted regions are in rocks essentially devoid of carbonaceous material. The observed provinciality is interpreted in terms of lateral heterogeneities in the lower crust supplying CO_2 to structures, represented by variations in the relative proportions of oxidised to reduced carbon, and implies that the faults are tapping very large crustal volumes.

Evidence from fluid inclusions concerning the properties of hydrothermal solutions involved in the fault-zone mineralisation is sparse, owing to pervasive transgranular fracturing and intracrystalline deformation of vein minerals. Some of the fluid-inclusion data is compiled in KERRICH (1983) and COLVINE (1984). Such fluids were of low salinity ($\leqslant 3$ wt-% NaCl equivalent), contained minor quantities of reduced gas species such as CH_4, CO, and COS, and minor N_2, possessed relatively high K/Na (0.1), and were characterised by variable CO_2 contents, probably signifying transient effervescence of CO_2 during decompression.

In the Timmins, Matheson, Kirkland Lake, and Val d'Or regions of the fault systems sulphates occur close to or within the structures. The sulphates, typically anhydrite or selenite, coexist with albite, magnesium-chlorite, calcite, and hematite. On the basis of stable-isotope data and mineralogical considerations these domains have been interpreted as sites for incursion of Archean marine water into submarine volcanic rocks along zones of high permeability, such as faults (KERRICH and HODDER, 1982; KERRICH and FYFE, 1983); ambient temperatures were 150 to 200 °C, and $\delta^{18}O$ fluid was 0 ± 1.5 per mil (Fig. 4A).

A third fluid regime is evident from stable-isotope data in plutonic rocks of the Kirkland Lake and Noranda districts. In these districts quartz-magnetite and quartz-chlorite veins were precipitated at temperatures of 120 to 250 °C from meteoric water of low ^{18}O (Fig. 4A).

Thus, cooling of the volcanic-plutonic complexes was initially dominated by ocean water, in the submarine environment, with a transition to devolatilisation of

large crustal volumes and, finally, to meteoric-water infiltration as the Archean volcanic-plutonic terrain emerged above sea level. This scheme is corroborated by the presence of late fluviatile clastic sediments.

2.5 *Age relationships*

A tightly constrained chronological framework exists for volcanic-plutonic activity in the Timmins and Kirkland Lake areas of the Abitibi greenstone belt, based on the classic uranium-lead isotopic age determinations conducted by KROGH and co-workers (Table 2). PERCIVAL and KROGH (1983) summarise the three-stage development of the Abitibi belt as a volcanic-sedimentary stage spanning 2750 to 2696 Ma, a metamorphic-tectonic event at 2700 to 2685 Ma, and late plutonism over the interval 2685 to 2665 Ma. The timing, however, of fluid transport through the major structures and the source of solute components have remained controversial issues.

Existing age determinations on mineralisation in such structures as the Kirkland Lake and Larder Lake fault zone are principally Stacey-Kramers model lead isotopic ages on galenas and leached coexisting pyrite, which define ages of 2656 to 2700 Ma (FRANKLIN et al., 1983). Rb–Sr isochron and incremental $^{40}Ar/^{39}Ar$ spectra yield closure times of 2550 to 2700 Ma; see Figure 5 (KERRICH et al., 1984; KERRICH, 1985). The least disturbed isotopic systems are in good agreement with model lead ages, whereas the younger ones reflect resetting during continued displacement along the major structures into the Proterozoic. For instance, the Kirkland Lake fault zone locally displaces Proterozoic Cobalt Group sediments, which are in the order of 2250 Ma.

According to these results in conjunction with field relations, marine water in-

Table 2

Age Constraints, Abitibi Belt

	Age (Ma)	
Timmins (NUNES and PYKE, 1981)		
Lower supergroup (top)	2725 ± 2	
Upper supergroup (top)	2703 ± 2	
Kidd Creek felsic host	2717 ± 4	
Kirkland Lake (NUNES and JENSEN, 1980)		
Hunter Mine group	2710 ± 2	
Blake River group	2703 ± 2	
Timiskaming		
Noranda		
Lake Dufault granodiorite	2701	
Abitibi batholiths (KROGH et al., 1982)	2675 – 2685	
Matachewan dykes (GATES and HURLEY, 1973)	2690 ± 93	$^{87}Sr/^{86}Sr = 0.700 \pm 0.001$

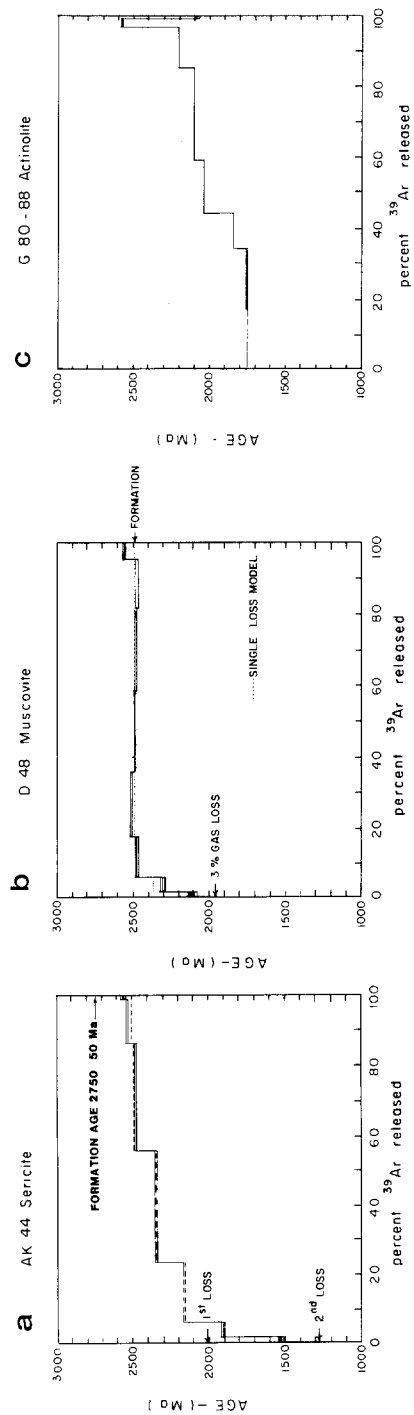

Figure 5
Incremental $^{40}Ar/^{39}Ar$ spectra from fault-related hydrothermal minerals. (a) Kerr Addison muscovite. (b) Dumagami muscovite. (c) Macassa actinolite.

cursion occurred along faults during early extension, but the dominant hydrothermal discharge in Abitibi belt fault zones is interpreted as having occurred during an episode of major fracturing and ductile deformation that accompanied emplacement of granitic batholiths into the supracrustal sequences; hydrothermal mineralisation was thus an integral part of the thermal and mechanical energy of the greenstone belt.

2.6 Source of hydrothermal solutes

The origin of fluid reservoirs that infiltrated structural lineaments has been considered above on the basis of light-stable isotope evidence. The source rock reservoir, however, for hydrothermally transported solutes, such as Si, CO_2, K, Rb, Li, Cs, Sr, and rare metals, including Au, Ag, As, Sb, B, Se, Te, Pb, Bi, and W, now present in mineralised faults, is a more subtle problem. The hypothesis of lateral secretion from wall rocks as the origin of mineralisation in fault zones formerly received wide acceptance (cf. BOYLE, 1961, 1979). Alternative hypotheses appeal variously with respect to granitic rocks, sediments, or komatiites as potential donor reservoirs. Herein the question of solute source is explored by means of radioisotope tracers, namely $^{87}Sr/^{86}Sr$, $^{207}Pb/^{204}Pb$, and $^{206}Pb/^{204}Pb$, which may be diagnostic of the specific rock reservoir from which the solutes were derived.

Contemporaneous $^{87}Sr/^{86}Sr$ ratios of the hydrothermally mineralised faults have been estimated from analyses of tourmaline, scheelite, and piemontite, all of which possess $^{87}Rb/^{86}Sr \leqslant 0.004$ and therefore have a negligibly small radiogenic-strontium evolution over the time elapsed since formation (Table 3). Moreover, these minerals, unlike ferrodolomites in the fault zones, appear to have behaved as isotopically closed systems.

If the estimated range of 0.7011 to 0.7040 for initial $^{87}Sr/^{86}Sr$ ratios of the source rock reservoir for hydrothermal solutes has validity, then this reservoir was more radiogenic than the upper mantle at 2690 Ma (0.700 ± 0.001), the Matachewan diabase dyke swarm which transects all major lithological units and structures (2690 ± 50 Ma, 0.701 ± 0.001), or the contemporaneous Abitibi belt volcanics of mafic to ultramafic composition (0.7000 to 0.7012); see Tables 2 and 3 and Figure 6 (FAURE, 1977; GATES and HURLEY, 1973; HART and BROOKS, 1974). An inferred radiogenic character for the source may implicate contributions from sialic basement to the greenstone belt, and/or felsic volcanic rocks of the Lower Supergroup, as well as volatiles released from the mafic to ultramafic volcanic sequence. FRANKLIN et al. (1983) have shown, on the basis of lead isotopic work, that in general fault-hosted gold mineralisation in the Abitibi greenstone belt possesses a characteristically more radiogenic signature and higher μ ($\mu = {}^{238}U/^{204}Pb$) than contemporaneous mafic volcanic rocks.

Thus the deduced Sr and measured lead isotopic characters of the fault mineralisation are more evolved than their contiguous mafic volcanic bounding media, collectively implicating an external, deeper-level, more radiogenic source of these

Table 3

Rb–Sr Isochron and $^{40}Ar/^{39}Ar$ Closure Ages for Mineralised Faults, and Age-corrected Mineral $^{87}Sr/^{86}Sr$

District, Mine	Age (Ma)	Method	$^{87}Sr/^{86}Sr$, initial	$^{87}Sr/^{86}Sr$, age-corrected	$^{87}Sr/^{86}Sr$ mineral, age-corrected *
Timmins					
Hollinger	2440 ± 26 2570 ± 30	Rb–Sr $^{40}Ar/^{39}Ar$ (muscovite)	0.70262 ± 0.0014	0.7015	
Parnour					0.7010 t
Paymaster					0.7012 to 0.7015 t
Aunor					0.7014 to 0.7020 t
Dome					0.7015 t, s
Kirkland Lake					
Macassa	2575 ± 50	$^{40}Ar/^{39}Ar$ (actinolite)			0.7012 to 0.7011 a, s
Kerr Addison	2510 ± 50 2550 ± 40	Rb–Sr $^{40}Ar/^{39}Ar$ (muscovite)	0.70249 ± 0.0009	0.7010	
Bousquet					
Dumagami	2420 ± 19 2550 ± 30	Rb–Sr $^{40}Ar/^{39}Ar$ (muscovite)	0.70406 ± 0.0001	0.7020	
Bousquet					0.7017 to 0.7019 t
Val d'Or					
Lamaque					0.7031 ± 0.7041 t
Pascales					0.7007 to 0.7014 t
Bras d'Or					0.7010 to 0.7022 t

* Abbreviations: t, tourmaline; s, scheelite; a, actinolite.

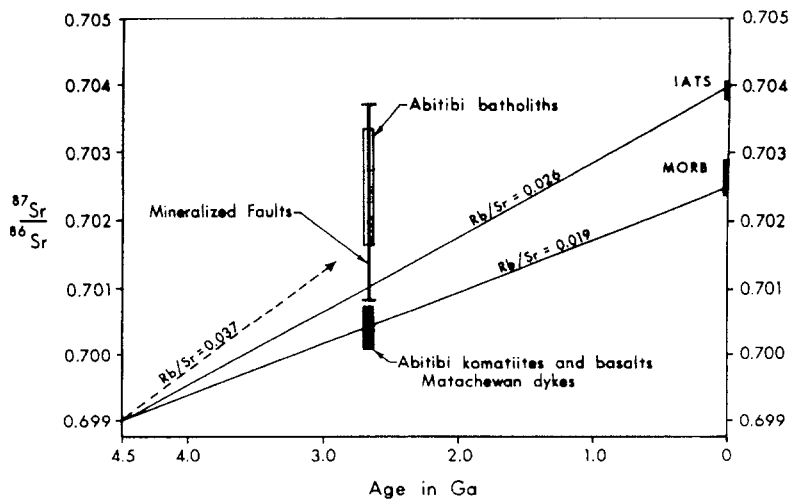

Figure 6

Contemporaneous $^{87}Sr/^{86}Sr$ of mineralised structures, compared with mantle, komatiites, and granodiorite batholiths, for the Abitibi greenstone belt at 2.7 Ga.

components. As a corollory, the lateral-secretion mechanism is ruled out. This inferred deeper source is plausibly the same as that donating Si, CO_2, K, Rb, Li, Cs, Au, Ag, As, Sb, B, etc. Long-range communication to a lower crustal source is corroborated by the presence of the major structures themselves, and also independent estimates of transport distances based on enrichments of rare elements in the structures (KERRICH and FRYER, 1979; KERRICH, 1983). Granulite facies rocks are typically depleted in LIL elements relative to the upper crust. The hydration and LIL-element enrichments observed in the faults may represent the discharged products of coeval devolatisation and depletion of LIL elements of the lower crust.

A distinct provinciality of $^{87}Sr/^{86}Sr$ initial ratios exists (Table 3) and, as in the case of regional variations in $\delta^{13}C$, this is interpreted in terms of large-scale lateral heterogeneity of the lower crust supplying volatiles and solutes to the structures.

2.7 Sodic and alkaline igneous rocks

A characteristic feature of the major fault zones, in addition to intense hydrothermal metasomatism, is the sporadically distributed colinear arrays of subvolcanic stocks, along with their extrusive equivalents, of highly sodic or alkaline composition (Fig. 1B). Prominent examples include trondhjemites of the Malartic, Matachewan, and Timmins areas, and alkaline rocks at Kirkland Lake (Fig. 1 A and B).

The sodic rocks are dominated by quartz and oligoclase or albite; they conform in most respects to the definition of a trondhjemite based on major-element oxides, according to BARKER (1979): SiO_2 at $>68\%$, usually $<75\%$, and Al_2O_3 typically at $>15\%$ at 70% SiO_2 and $<14\%$ at 75% SiO_2, and Na_2O at 4.0–5.5% (etc.). For instance, a population of six trondhjemites at Canadian Arrow possesses SiO_2 at $65.9 \pm 1.81\ 1\sigma$, Al_2O_3 at $16.7 \pm 0.22\ 1\sigma$, and Na_2O at $8.32 \pm 1.16\ 1\sigma$ (MCNEIL and KERRICH, 1985). Most such trondhjemites have elevated primary Na_2O contents, but this is incremented during pervasive spilitic alteration in the presence of marine water, under conditions of low temperature, as evidenced by reversed quartz-feldspar fractionations ($\delta^{18}O$ for quartz, 9 to 11, and $\delta^{18}O$ for albite, 10 to 16; FRYER et al., 1979; KERRICH and FRYER, 1979; KERRICH, 1983).

Groups of alkaline igneous intrusions and trachytic tuffs are abundant at Kirkland Lake; formerly termed 'syenites', these rocks are in fact potassic basalts and intrusive equivalents. A general consensus exists that alkaline mafic rocks are the products of low degrees of partial melting of asthenosphere, or 'enriched' asthenosphere, and such fusion products may have a preferred spatial association with linear fracture zones, such as rifts (cf. FITTON, 1985). Along with the alkaline magmas are lamprophyre dykes and domains of fenitisation, highly enriched in large-ion lithophile elements. Representative chondrite normalised diagrams are depicted in Figure 7, (A) to (D); a characteristic feature of the alkaline rocks is the pronounced chondrite-normalised troughs at Ta–Nb, P, and Ti; see Figure 7, (C) and (D). Magmas of trondhjemitic composition are generally regarded as having been formed by a partial

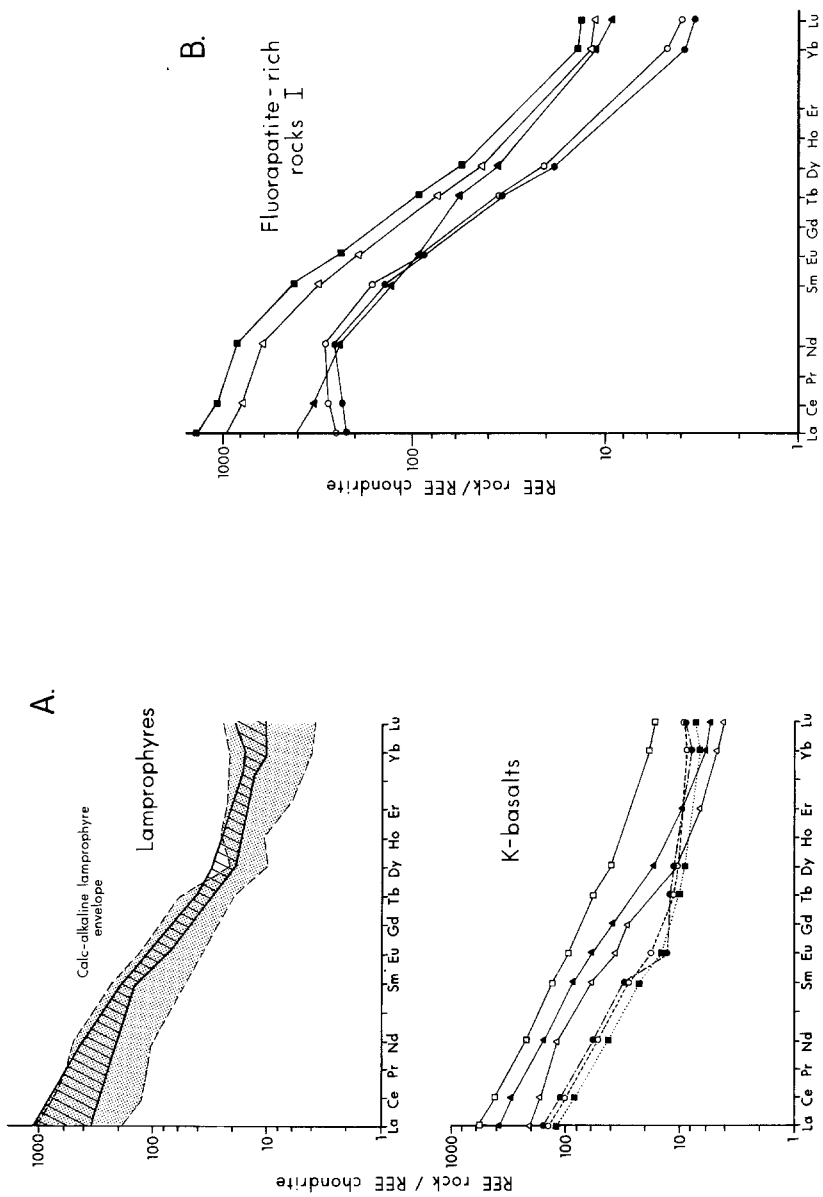
A.
Lamprophyres
Calc-alkaline lamprophyre envelope
K-basalts
B.
Fluorapatite-rich rocks I
REE rock / REE chondrite
1000
100
10
1
La Ce Pr Nd Sm Eu Gd Tb Dy Ho Er Yb Lu

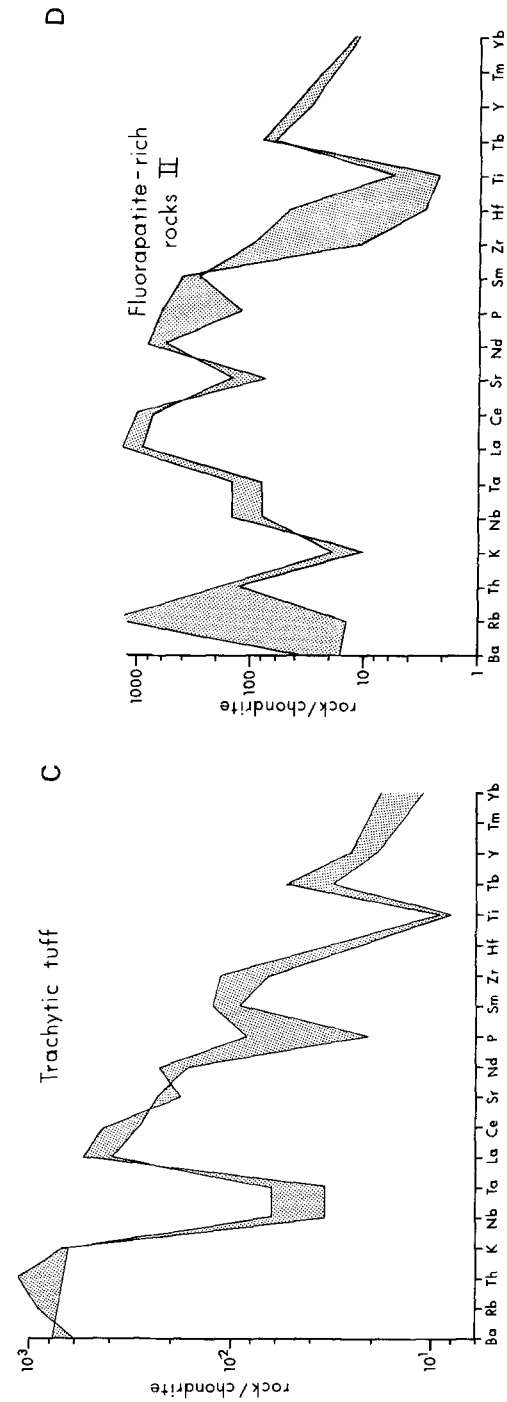

Figure 7

Chondrite normalised element distributions for specified suites of alkaline magmas. (A) Lamprophyres diagram, after McNeil and Kerrich, 1986; alkali-basalts diagram, after Kerrich and Watson, 1984. (B) Fluorapatite-bearing fenitised trondhjemites, from King, 1983; trachytic tuffs (Kirkland Lake) and fluorapatite-rich fenites, after Kerrich and Watson, 1984, and King, 1983, respectively.

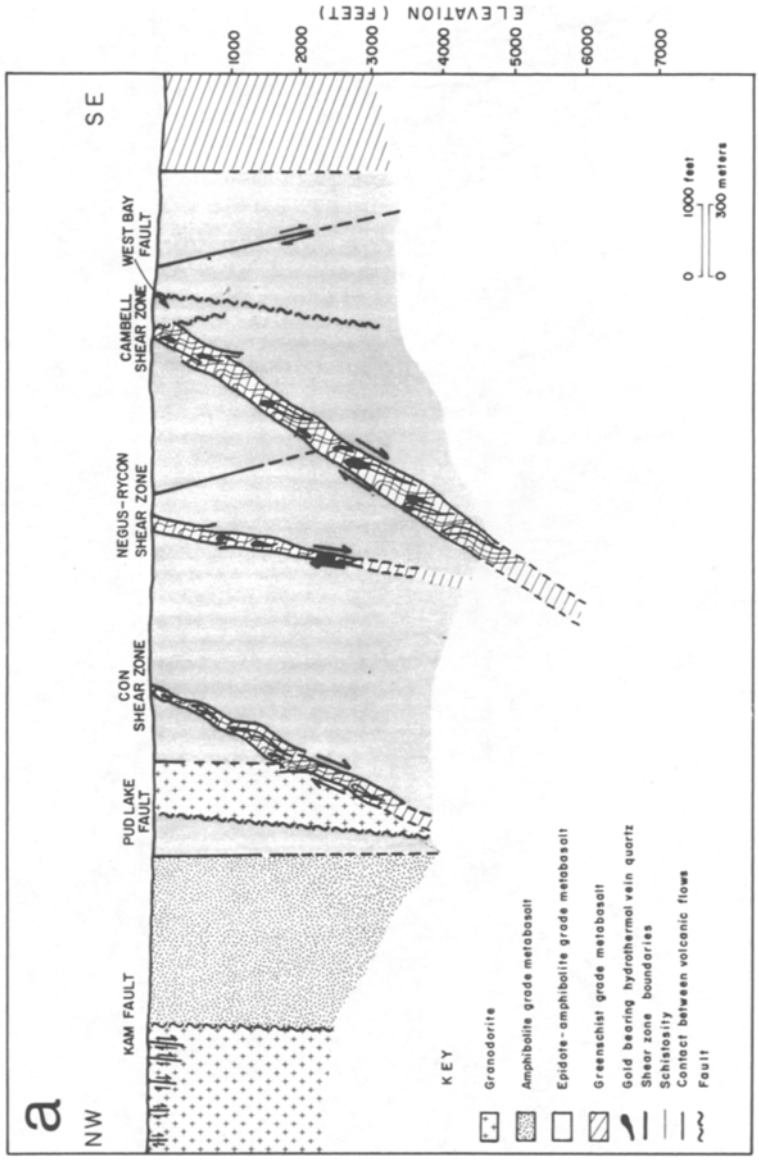
a
NW
SE
KAM FAULT
PUD LAKE FAULT
CON SHEAR ZONE
NEGUS-RYCON SHEAR ZONE
CAMBELL SHEAR ZONE
WEST BAY FAULT
ELEVATION (FEET)
1000
2000
3000
4000
5000
6000
7000
0 1000 feet
0 300 meters
KEY
Granodorite
Amphibolite grade metabasalt
Epidote-amphibolite grade metabasalt
Greenschist grade metabasalt
Gold bearing hydrothermal vein quartz
Shear zone boundaries
Schistosity
Contact between volcanic flows
Fault

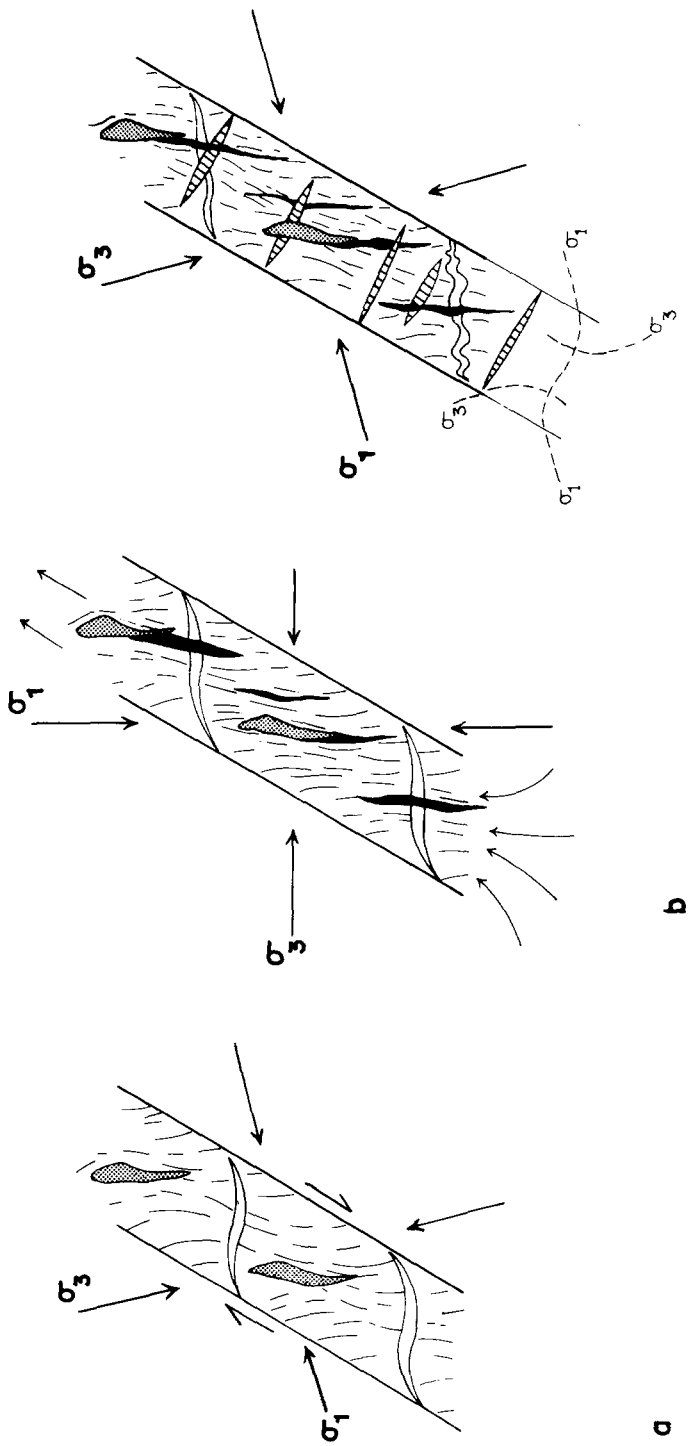

Figure 8
(a) Schematic geological cross section of Yellowknife greenstone belt, illustrating disposition of principal rock types and geometry of brittle–ductile shear zones. (b) Possible switching of stress regimes accompanying hydraulic fracturing and generation of the three sets of vein arrays. After KERRICH and ALLISON, 1978.

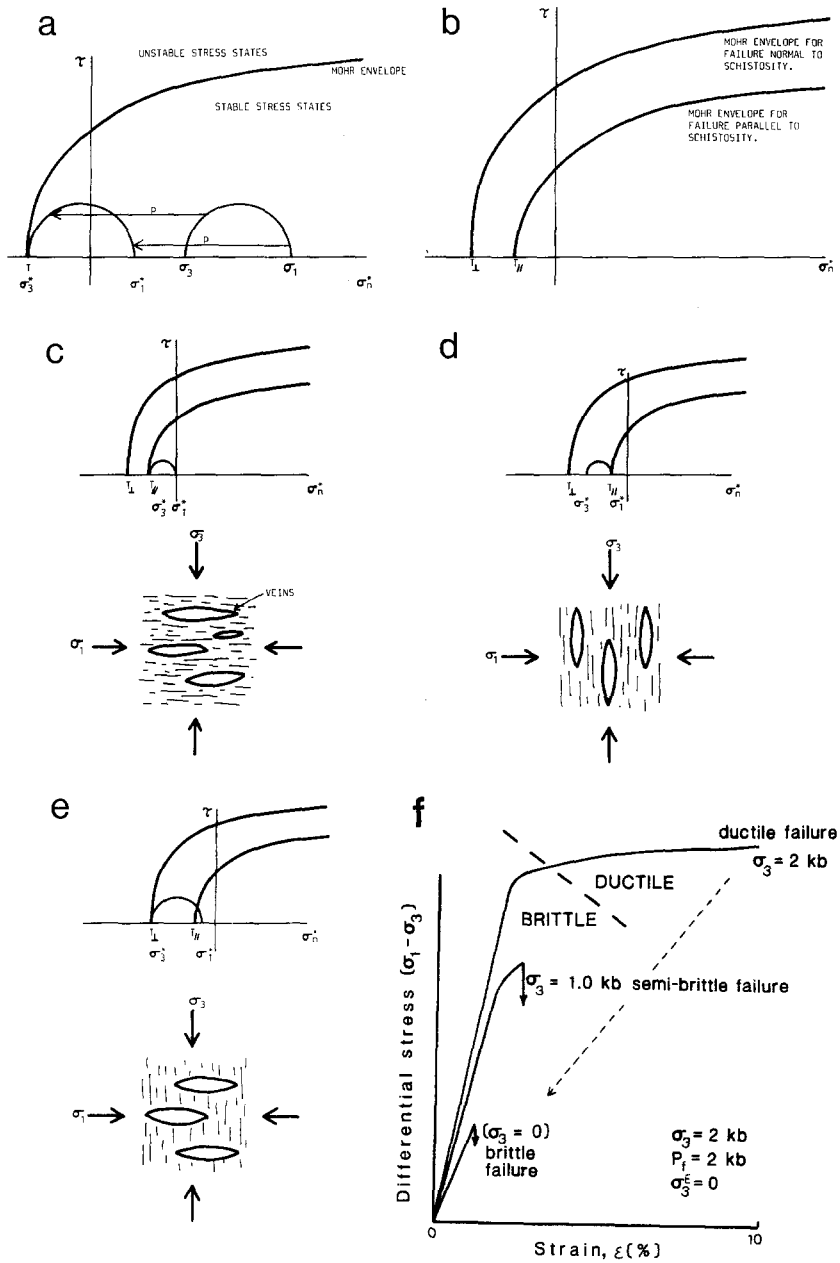

Figure 9

Mohr diagrams illustrating inferred stress conditions for formation by hydraulic fracturing of en-echelon veins of first stage; effective normal stresses $\sigma_n = \sigma_n - p$ versus shear stresses τ. (a) Mohr's stress semicircle at left represents external stress condition; semicircle at right, external stresses modified by fluid pressure p at failure. Mohr envelope is that of Griffith criterion in tensile regime and of Navier-Coulomb criterion in compressive region of diagram; T is tensile strength of undeformed metabasalt. Note that all diagrams are symmetrical across the $\tau = 0$ line. (b) Failure parallel and normal to schistosity: $T_\perp$ and $T_\parallel$ are

melting of mafic granulites at the base of the greenstone belt sequence (COLLERSON and FRYER, 1978; BARKER et al., 1979).

The spatial association of trondhjemites and alkaline magmas with major linear structures is interpreted in terms of translithospheric fractures, which tap magmas of sodic composition generated at the base of the crust, and deep asthenospheric partial melts of alkaline composition. Such magmatic activity is broadly coeval with venting of hydrothermal fluids, the latter probably from a crustal reservoir; thus magmatism, tectonic activity, and fluid motion are all linked to a thermal anomaly.

2.8 Hydraulic conditions during vein propagation

One of the fundamental questions pertaining to mineralised Archean faults is the hydraulic regime of the fluid system. Are the geothermal fluids undergoing thermally driven convective circulation under approximately hydrostatic conditions and in equilibrium with surface waters or, alternatively, do the extensive vein stockworks form by hydraulic fracturing in the presence of geopressurised aqueous reservoirs? This question has been addressed by KERRICH and ALLISON (1978) and ALLISON and KERRICH (1979) with reference to Yellowknife, and by ROBERT and BROWN (1984) for the Sigma Mine, Val d'Or, where orientations of the principal stresses and ambient fluid pressures during vein propagation may be deduced, given the well-constrained geometry of shear zones and the vein arrays they host.

A three-stage sequence of veining has been recognised in major brittle–ductile shear zones of the Yellowknife greenstone belt (KERRICH and ALLISON, 1978; ALLISON and KERRICH, 1979), as follows.

1. Formation of the major shear zones, with concomitant development of the early en-echelon barren veins.
2. Development of the massive to banded gold-quartz veins approximately parallel to the schistosity, in the shear zones.
3. Formation of late 'ladder' vein systems, which are also locally auriferous, at high angles to the schistosity within the shear zones.

---

uniaxial tensile strengths of schist. (c) Hydraulic fracturing parallel to schistosity when it is oriented normal to the σ_3 direction. This is one limiting case; the other is shown in Figure 8. (d) Hydraulic fracturing across a plane perpendicular to schistosity when σ_1 direction is normal to this plane; this will occur only if $\sigma_1 - \sigma_1 \leqslant T_\perp - T_\parallel$. (e) Inferred stress conditions for development of late 'ladder' veins: differential stress exceeds difference in strengths of schist parallel and perpendicular to schistosity. After ALLISON and KERRICH, 1979. (f) Generalised rheological behaviour of rock, illustrated in differential stress, $\sigma_1 - \sigma_3$, versus strain, coördinate space. Note transition from brittle to ductile behaviour at elevated values of confining stress σ_3; the transition can be induced by transient increases of fluid pressure which act to diminish effective confining stress, $\sigma_3 - P_{\text{fluid}}$.

This sequence is illustrated in Figure 8b. The origin of each vein system will now be considered in turn.

The veins at Yellowknife were formed by the infilling of tensile fractures. Close to the Earth's surface tensile fractures may be formed, but at depth the increase of confining pressure σ_3 induces propagation of shear fractures. Under conditions of high fluid pressure P_f, however, tensile failure by hydraulic fracturing may occur in the crust at depths in excess of 30 km. The principles involved are discussed by FYFE et al. (1978). The stress conditions under which hydraulic fracturing can occur may be represented by

$$\sigma_3 - P_f \leqslant T$$
$$\sigma_1 - \sigma_3 \leqslant -4T$$

where σ_1 and σ_3 are the maximum and minimum principal stresses respectively and T is the tensile strength of the rock. The first inequality represents the condition where the fluid pressure exceeds the confining pressure by an amount equal to or greater than the tensile strength of the rock. The second inequality is the condition for suppression of the shear failure mode. These stress conditions may be portrayed on a Mohr diagram (Fig. 9a).

The shear zones are characterised by an intense schistosity, the mechanical properties of which are highly anisotropic. In particular, the tensile strength in a direction normal to the schistosity, $T_\perp$, will be low compared with that parallel to the schistosity, $T_\parallel$. On a Mohr diagram the envelope for failure parallel to the schistosity will appear at lower stresses than the envelope for failure normal to the schistosity (Fig. 9b). As the pore-fluid pressure increases, however, and the effective stresses are reduced until σ_3 intersects the Mohr envelope, failure will occur only if the schistosity is oriented normal to the direction of σ_3 (Fig. 9c). If the schistosity is oriented orthogonal to the σ_1 direction, then failure along the schistosity will occur when the value of σ_1 intersects the Mohr envelope, as long as σ_3 is less than the tensile strength of the rock normal to the schistosity (Fig. 9d). It is thus possible to achieve hydraulic fracturing within the shear zone parallel to the schistosity with the same external stress regime that caused the initial development of the shear zones, and the switch in orientation of stresses, postulated by KERRICH and ALLISON (1978) and illustrated in Figure 8b, is plausible, but not necessary. The stress conditions that must be satisfied for these veins to develop are the following.

$$\sigma_3 - P_f \leqslant T_\parallel)$$
$$\sigma_1 - \sigma_3 < -(T_\perp - T_\parallel)$$
$$\sigma_1 - \sigma_3 \leqslant -4T_\parallel$$

The latest system of fractures occurs as an array of 'ladder' veins oriented approximately normal to the schistosity and dipping at shallow angles towards the east. These veins cross-cut those of the second stage, which now have a pinch and swell structure as a result of progressive incremental deformation in the shear zones.

The stress conditions for this late stage of hydraulic fracturing may be formulated as

$$\sigma_3 - P_f \leqslant T$$
$$\sigma_1 - \sigma_3 < -4T$$
$$\sigma_1 - \sigma_3 < -(T_\perp - T_\parallel)$$

and are portrayed on the Mohr diagram as in Figure 9e.

The geometry of the early veins and the schistosity within the shear zones accords well with the concept of shear-zone development in rocks showing material behaviour that is transitional between brittle and ductile.

The geochemical evidence indicates local redistribution of material via migration in a fluid phase and the absence of any significant mineralisation during the initial development of the ductile shear-zone structures. The second-stage veins have a conspicuous banding and often contain slivers of schist oriented parallel to the vein margins. Later intracrystalline deformation has largely obliterated the original quartz microstructure, but the banded nature of the veins and the volumes of hydrothermal fluids involved suggest that the veins were formed by repeated hydraulic fracturing and infilling by quartz precipitated from the hydrothermal fluids. One may envisage a repeated cycle of buildup of a fluid reservoir accompanied by elevation of fluid pressure to a point sufficient to induce hydraulic fracture, leading to discharge of the geopressurised reservoir, with a resultant volume increase and a consequent reduction of fluid pressure in the source region. Repeated episodes of hydraulic fracturing under conditions of high P_f have cycled the effective confining stress ($\sigma_3 - P_f$) such that the rocks have in turn cycled through the brittle ($\sigma_3 - P_f$, low) to ductile ($\sigma_3 - P_f$, high) transition (Fig. 9f).

Mechanical anisotropy of schists within the shear zones will cause refraction of the stress, and hydraulic fracturing will tend therefore to form parallel or normal to the fabric as in the second and third stages of vein development (Fig. 8 and 9).

Development of the second-stage veins requires fluid pressure to exceed the maximum principal stress by an amount equal to the tensile strength. This will occur if the fluid pressure has a value close to the geostatic pressure for a given depth. Hydraulic fracturing will permit upward movement of this fluid, the pressure of which is equivalent to the geostatic pressure at greater depth minus the hydraulic gradient, and which, we suggest, is capable of exceeding the maximum principal stress at higher levels (Fig. 8). The hydraulic fractures will therefore propagate from depth towards the surface.

These structural considerations apply equally to many other examples of the fault-hosted mineralisation discussed above, which also appear to have formed under conditions of hydraulic fracturing induced by geopressurised hydrothermal reservoirs.

3. *Grenville front*

The Grenville front, near Coniston, Ontario, is defined by the Grenville front boundary fault and associated mylonite zones. These structures collectively form the demarcation between low-grade metasediments of the southern province and high-grade Grenville gneisses (LA TOUR, 1981). Translation on the fault zone is thought to be of Grenville age ($\approx$1100 Ma), although the magnitude and direction of displacement are not precisely known. Bordering these structures immediately to the north is a major fault, the Wanapitae.

LA TOUR (1981a) has distinguished two discrete and distinct mylonite zones at the Grenville front, designated MZI and MZII respectively. Metamorphic reactions associated with MZII are prograde in nature. On the basis of garnet-biotite geothermometry the ambient temperature of deformation is estimated at 600 °C, and oxygen isotope fractionations (Δquartz-muscovite is 2.6 to 2.8 per mil) yields temperatures of 580 to 640 °C, in close accord with that given above (KERRICH et al., 1984). The $\delta^{18}O$ of quartz in mylonitic schists is uniform at 11.0 to 11.8; syntectonic quartz veins have $\delta^{18}O$ values within the same range as quartz in the host rock, signifying a growth of veins in isotopic equilibrium with schists, probably from the same fluid. Fluids present during syntectonic veining and deformation have a calculated $\delta^{18}O$ of 9.6 $\pm$ 0.6.

Metamorphic reactions in mylonite zone MZI are exclusively retrograde in nature, and garnet amphibole thermometry indicates that deformation occurred at temperatures below 540 °C (LA TOUR, 1981). Oxygen isotope data for MZI yield temperature estimates of 420 to 490 °C and fluid isotopic compositions of 7.0 $\pm$ 0.6 per mil. Fluids present during deformation along MZII and MZI were probably of metamorphic origin, indigenous to the immediate host rocks.

Rock units transected by the Wanapitae fault have undergone extensive brittle fracturing, accompanied by local quartz-albite-carbonate veining. Oxygen isotope data on cataclastically deformed metadiabase yields temperature estimates of 280 $\pm$ 40 °C, and a fluid $\delta^{18}O$ of +3.2. Fluid involvement in the Wanapitae fault was at relatively low temperatures, possibly from a reservoir of formation brines (KERRICH et al., 1984).

An array of quartz-hematite veins ($\delta^{18}O$ for quartz of -0.8 to -1.3) occupies fracture arrays superimposed on the mylonitic fabric of MZI. Quartz crystallised at temperatures of 200 to 350 °C in the presence of fluids of low ^{18}O with an isotopic composition of -8 (350 °C) to -14 (200 °C) per mil. Continental meteoric water is the only terrestrial fluid reservoir with negative $\delta^{18}O$ (TAYLOR, 1974). The fluid $\delta^{18}O$ values calculated above are commensurate with that of precipitation on high mountain ranges at mid to high latitudes, such as the Sierra Nevada, Rocky, or Andean mountains (cf. TAYLOR, 1974). This episode of fracturing is interpreted as having) resulted from the infiltration of waters with low ^{18}O derived from precipitation on a high mountain range, down a brittle fault zone. The mountain range

could have been induced by continental collision, with deformation accompanying crustal thickening accommodated at deep levels by translation on the high-temperature mylonite zone MZII, followed by isostatic rebound on the low-temperature zone MZI and the associated Grenville front boundary fault (LA TOUR, 1981; KERRICH et al., 1984). This scheme could account for the tectonic juxtaposition of high-grade gneisses that had been deformed in a ductile mode in the presence of metamorphic fluids at elevated temperatures and low-grade metasediments that had experienced brittle fracturing during the incursion of an ^{18}O-depleted surface reservoir.

4. Shear-zone-hosted uranium in overthrust Archean gneisses, Bahia, Brazil

Ductile shear zones transecting high-grade Archean basement gneisses over a band 40 by 100 km near Lagoa Real, State of Bahia, Brazil, are host to extensive uranium mineralisation. The mineralisation is associated with retrograde metamorphism and extensive sodium metasomatism of host felsic gneissic basement rocks (LOBATO et al., 1983, a, b, c). Preliminary oxygen isotope studies of the uranium deposits together with their host gneisses revealed that the uraninite was precipitated from hydrothermal solutions of meteoric origin ($\delta^{18}O \leqslant -2$ per mil) at temperatures of $\approx 550\,^{\circ}C$; see Figure 10A (LOBATO et al., 1983, a, b, c).

A model in which amphibolite and granulite facies basement gneisses were transported over Proterozoic greenschist facies metasediments of the Espinhaço sequence along a thrust surface has been proposed by those authors (LOBATO et al., 1983, a, b, c). Such a mechanism involving tectonic emplacement of portions of hot basement over colder, wet rocks would induce dehydration and overpressure in meteoric-water-charged aquifers, causing the high fluid pressures necessary to maintain thrust motion (cf. FYFE et al., 1978).

Calculated or measured $\delta^{18}O$ and δD values of hydrothermal solutions implicated in the mineralisation can provide information on the original fluid reservoir. Identifying the rock reservoir(s) that donated metals to any specified deposit, however, is a more subtle and less tractable problem. The question of uranium provenance for the shear-zone-hosted uraninite deposits has been addressed by means of Rb/Sr isotopic tracer studies. Coenrichment in strontium and uranium during hydrothermal alteration can be deduced on the basis of mineralogical and textural relations and chemical mass balance in the shear zones, but this does not necessarily imply that uranium and strontium have been leached from a common rock reservoir. Despite this, strontium isotope tracer studies can constrain the possible rock reservoirs with which the hydrothermal solutions equilibrated.

Four possible strontium donor reservoirs may be envisaged: Archean gneisses, Proterozoic rocks, seawater, and alkalic intrusive rocks. The Archean gneisses have a Rb/Sr isochron age of 2.86 Ga (CORDANI, 1982) and an elevated Rb/Sr ratio and

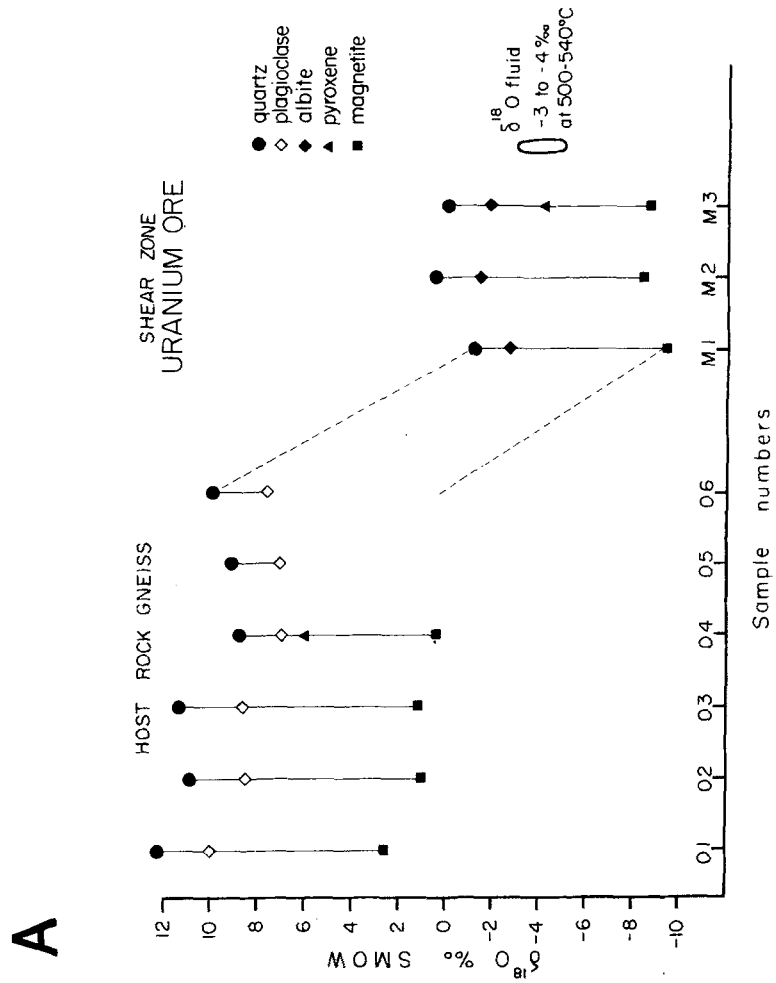
A
HOST ROCK GNEISS
SHEAR ZONE
URANIUM ORE
quartz
plagioclase
albite
pyroxene
magnetite
δ18O fluid
-3 to -4‰
at 500-540°C
MOWS ‰ δ18O
12
10
8
6
4
2
0
-2
-4
-6
-8
-10
01
02
03
04
05
06
M1
M2
M3
Sample numbers

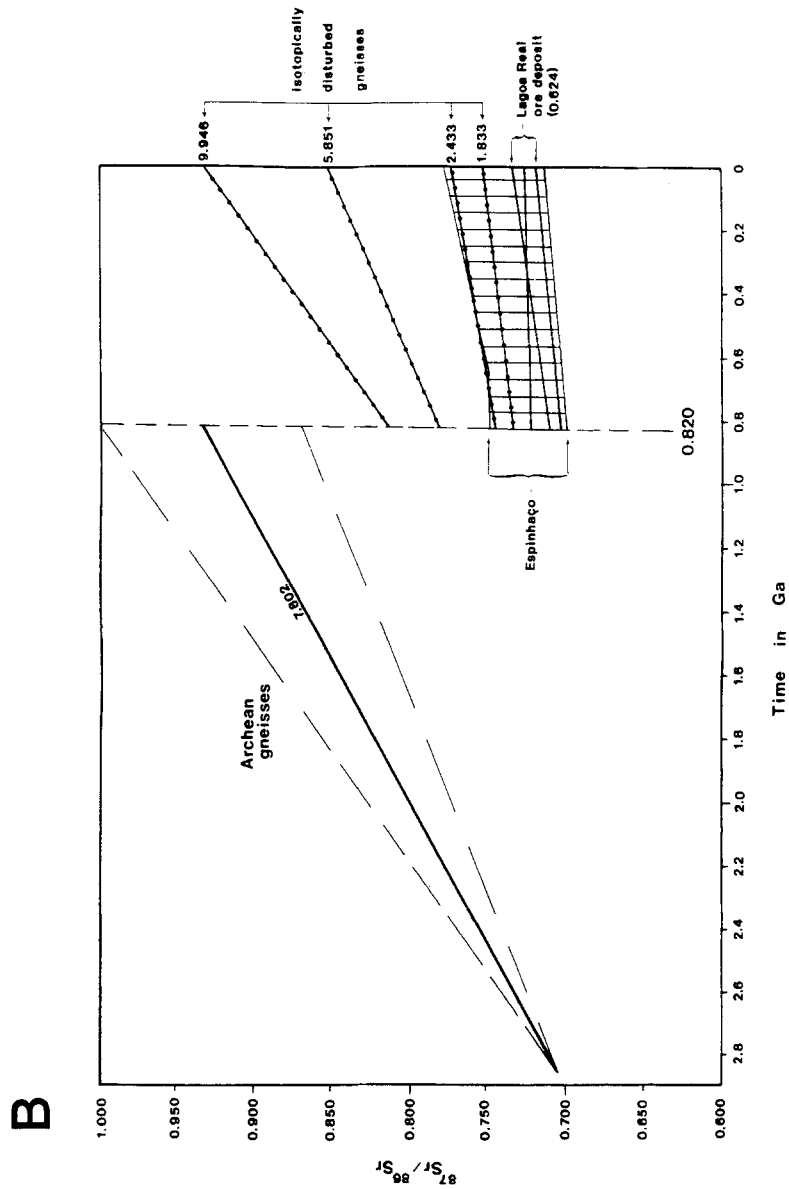

Figure 10
(A) The $\delta^{18}O$ of specified minerals in shear zones and wall rocks, Lagoa Real, Brazil. After LOBATO et al., 1983, b. (B) The $^{87}Sr/^{86}Sr$ of specified rock reservoirs at Lagoa Real, Brazil. After KERRICH et al., 1986. See text for explanation.

therefore have evolved along a steep $^{87}Sr/^{86}Sr$ trajectory through time. The Espinhaço sequence is substantially younger, with a Rb/Sr isochron age of 1.0 Ga for volcanic rocks of the Boquira Formation. Hydrothermal alteration of deformed gneisses accompanying uraninite deposition resulted in an almost total loss of rubidium with concomitant gains of strontium (LOBATO et al., 1983c). Thus the Rb/Sr ratios in the deposit and its altered host rock are <0.01, such that little ^{87}Sr has evolved.

Establishing the source of strontium in the uranium deposit requires a knowledge of the mean $^{87}Sr/^{86}Sr$ ratio of each of the possible donor reservoirs at the time of uranium introduction. The best current estimate of the age of uranium mineralisation is 820 Ma, according to $^{207}Pb/^{206}Pb$ age determination (STEIN et al., 1980). An average value for the $^{87}Sr/^{86}Sr$ ratio of the gneisses at 820 Ma can be estimated from isochron data (CORDANI, 1982). From the average $^{87}Rb/^{86}Sr$ (7.8), the initial $^{87}Sr/^{86}Sr$ ratio at the time of last strontium isotope homogenisation (0.705 at 2.86 Ga), and the elapsed time to mineralisation, a mean $^{87}Sr/^{86}Sr$ of 0.935 at 820 Ma is obtained. This assumes that the samples used in constructing the isochron are representative of the gneisses as a whole. An array for the strontium isotope evolution of the gneisses is portrayed in Figure 10B, calculated from the mean $^{87}Rb/^{86}Sr$ and Rb/Sr $\pm$ 2 of the mean (KERRICH et al., 1986).

A second approach to estimating the $^{87}Sr/^{86}Sr$ of the gneisses at 820 Ma is by means of a suite of samples collected from the vicinity of orebodies but external to the shear zones. Back-extrapolation of analytically determined $^{87}Sr/^{86}Sr$ ratios, with the use of measured $^{87}Rb/^{86}Sr$, gives a mean of 0.770 at 820 Ma. This second estimate is significantly lower than that calculated from the isochron data and is interpreted as reflecting a lowering of the $^{87}Sr/^{86}Sr$ ratio of the gneisses by an infiltration of hydrothermal fluids with relatively low $^{87}Sr/^{86}Sr$ during uranium mineralisation; see Figure 10B (KERRICH et al., 1986).

At 820 Ma the Proterozoic Espinhaço had a calculated range in $^{87}Sr/^{86}Sr$ of 0.700 to 0.740 and a mean of 0.732. Though slightly higher, this ratio is close to that of the uranium deposit (Fig. 10B). Contemporaneous marine water was 0.708 (VEIZER and COMPSTON, 1974). Measured $^{87}Sr/^{86}Sr$ ratios of the ore deposit are uniform, in keeping with their low Rb/Sr ratios. The deposit is projected to have been characterised by an $^{87}Sr/^{86}Sr$ of 0.719 at 820 Ma. Strontium evolution arrays are depicted for all of the rock reservoirs considered in Figure 10B. From these data it is clear that at 820 Ma the Proterozoic Espinhaço had an $^{87}Sr/^{86}Sr$ ratio close to that of the uranium deposit.

Other possible rock reservoirs cannot be ruled out as strontium donors, and mixtures of strontium from seawater and the gneisses remains an alternative explanation. If this is taken in conjunction, however, with constraints imposed by field relations, mineralogy, and $^{18}O/^{16}O$ data, the conclusion is that strontium in the orebody was originally indigenous to the Proterozoic Espinhaço, having been transported to the site of deposition by high-temperature hydrothermal fluids originating

as formation brines in the Espinhaço and discharged through shear zones in response to the thrust mechanism, as discussed by LOBATO et al. (1983, a, b). Estimates of the fluid volume discharged are ≈ 1000 km^3 on the basis of considerations of uranium solubility.

5. *Metamorphic core-complex detachment faults*

Metamorphic core complexes constitute an unique structural entity in the tectonic architecture of the North American Cordillera. They are broadly domal physiographic features, characterised geologically by a basal core of intensely deformed metamorphic and/or plutonic rocks, grading upwards through mylonitic equivalents to low-angle planar breccia zones delimiting a detachment fault. This 'infrastructure', or lower plate, is overlain by a 'suprastructure', or upper plate, composed of listrically faulted, allochthonous, and generally unmetamorphosed Tertiary rocks (for an overview see (CONEY, 1980). Twenty-five such core complexes have been identified to date, discontinuously arrayed along the axis of the North American Cordillera (CONEY, 1980).

Chloritic breccias, characterised by pervasive transgranular fracturing, propylitic alteration, and hydraulic fractures occupied by veins, superimposed on the mylonitic rocks, are a prominent feature of metamorphic core complexes. Breccia zones are coplanar with detachment faults, which are also the sites for local Cu–Au mineralisation, with associated vein networks bearing hematite and manganese oxide. These features raise questions as to the nature of the fluid regimes responsible for metasomatic alteration and fracturing along the plane of detachment.

The Picacho Mountains are located near Phoenix in southern Arizona and constitute the southerly extension of the array of metamorphic core complexes aligned along the North American Cordillera (CRITTENDEN et al., 1980). Geological descriptions of the area are given by several authors, most recently by REHRIG and KEITH (1984). The geological relations of the Picacho area resemble those of a typical metamorphic core complex; see Figure 11 (cf. CRITTENDEN et al., 1980). The key geological components are three tectonic plates, or thrust blocks, separated by two intervening detachment thrusts. Undeformed to mylonitic granite of the lower plate is demarked by a lower detachment thrust, underlain by chloritic breccia. Variably altered and fractured granitic rocks of the middle plate are bounded by an upper detachment zone, upon which allochthonous volcanic and sedimentary rocks of Miocene age lie (Fig. 11). The volcanics have experienced intensive low-temperature oxidative alteration, such that the dominant secondary minerals are K-feldspar, calcite, hematite, and manganese oxides.

At the Picacho tectonic section the salient isotopic features are an upwards trend of whole-rock $\delta^{18}O$ from 7.6 to 18.9 in conjunction with a decrease of estimated ambient temperature from 550 to 150 °C (Fig. 11, A, B). In undeformed Oracle

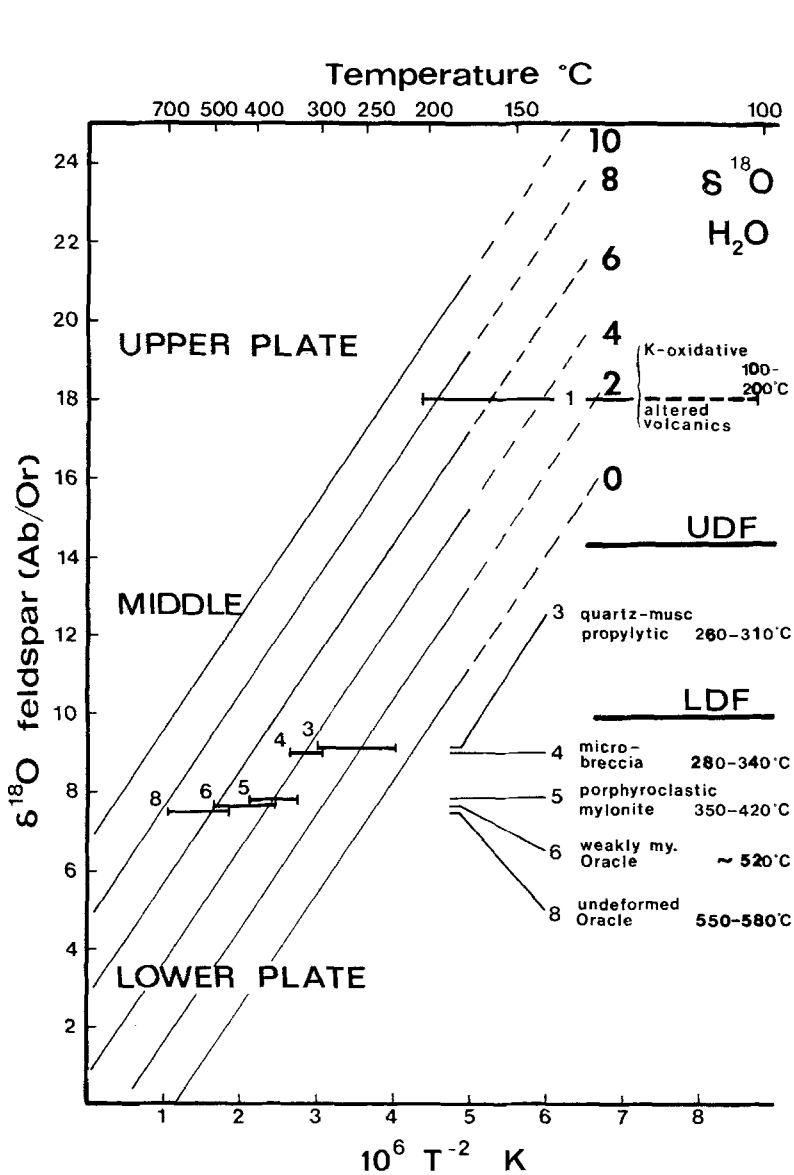

granite of the lower-plate quartz ($\delta^{18}O$, 9.1 to 10.8 per mil), feldspar (7.5 to 8.2) and hornblende (4.9 to 5.6) possess near-magmatic isotopic fractionations. The calculated isotopic temperatures are 500 to 600 °C. A calculated $\delta^{18}O$ of H_2O in equilibrium with feldspars of about +7 is appropriate for magmatic fluids of granites with normal $\delta^{18}O$ (Fig. 11A).

Mylonitic counterparts of the Oracle granite within the lower plate have a small

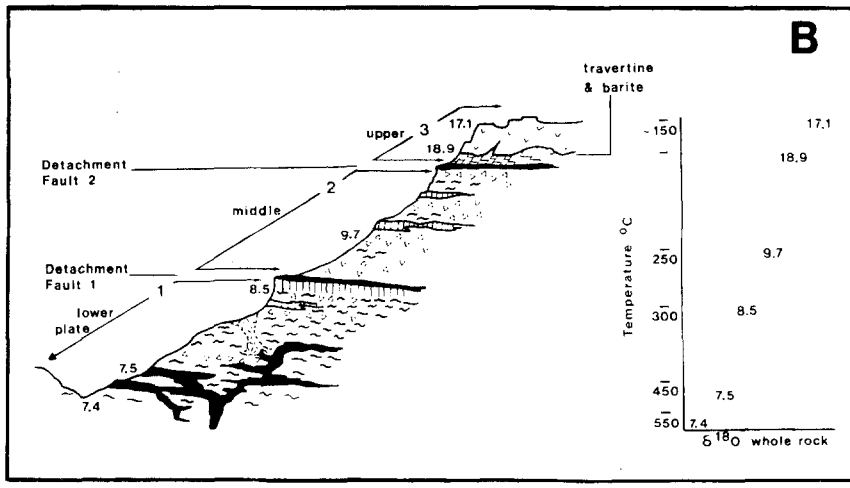

Figure 11

(A) The ^{18}O of feldspar versus temperature, estimated on basis of mineralogical criteria and oxygen isotope fractionations for Picacho section. Family of lines represents $\delta^{18}O$ of water in equilibrium with albite or K-feldspar of specified $\delta^{18}O$ at given temperatures. (B) Tectonic cross section with measured $\delta^{18}O$ of whole rock. Note increase of $\delta^{18}O$ up section. After KERRICH and REHRIG, 1986.

but systematic ^{18}O shift in quartz relative to their undeformed precursors; accordingly, the quartz-feldspar fractionations are larger. The calculated isotopic temperatures are 350 to 500 °C; these are regarded as a dynamic and metamorphic overprint of the granitic protolith and pertain to the ambient thermal conditions of mylonite formation. Whole-rock oxygen isotope compositions of the mylonitic rocks are identical with undeformed Oracle granite, within the limits of analytical uncertainty. Hence the mylonites probably developed under conditions of low water-to-rock ratio in the presence of fluids derived from a breakdown of hydrous minerals in the granitic precursor. The $\delta^{18}O$ of these fluids is calculated at 3 to 6 per mil, and they probably are predominantly of metamorphic or magmatic origin or evolved formation brines, or all three reservoirs.

Brecciated mylonite, which underlies the lower detachment surface, has a quartz $\delta^{18}O$ of 11.6 and thus has experienced a positive ^{18}O shift of $+2.3$ per mil relative to quartz in the underlying ductile mylonitic precursors of the breccia. Fractionations amongst quartz, feldspar, and chlorite correspond to isotopic temperatures of 300 to 350 °C. The positive shift in quartz is accompanied by a whole-rock shift of $+1$ per mil relative to mylonitic and pristine Oracle granite; these relations require that the breccia has experienced fluid fluxing, in order to account for the measured isotopic excursion. Hydrothermal fluids in equilibrium with the chlorite breccia have a calculated $\delta^{18}O$ of 4 ± 1. Thus the breccia marks a structural-hydrological domain representing the boundary from a lower zone of low water-to-rock ratio to an upper zone of high fluid fluxes.

Veined and hydrothermally altered rocks of the middle plate have elevated quartz $\delta^{18}O$ (12 per mil) and whole-rock values (9.7 per mil) relative to the underlying plate and thus define a progressive trend of ^{18}O enrichment up the structural section. The temperatures of alteration are estimated to be 220 to 330 °C in the presence of a fluid $\delta^{18}O$ of 2 to 5 per mil.

The temperatures of hydrothermal alteration in volcanic rocks of the upper plate cannot readily be estimated. Assuming a span of 100 to 200 °C, fluids of -3 to $+8$ per mil are implicated in the oxidative event that produced K-feldspar, illite, hematite, carbonate and manganese oxides.

In summary, upwards in the tectonic section temperatures progressively diminish and the whole-rock $\delta^{18}O$ increases dramatically. These relations are interpreted as signifying dual fluid regimes: expulsion of high temperature, crust-equilibrated and reduced fluids of metamorphic, magmatic, or formation origin from lower structural levels, through the middle plate, accompanied by cooling, in contrast to cool, oxidising thermal waters into the upper plate. Thus the tectonic section records an upward transition from high to low ambient temperature, low to elevated water-to-rock ratio, ductile to brittle deformation, and a fluctuating interface of deep aqueous reservoirs at lithostatic pressure, with shallow surface ones under hydrostatic conditions.

6. Summary and conclusions

In general, fluid regimes in the fault and shear zones studied follow a sequence, from conditions of high temperature and pressure with locally derived fluids at low water-to-rock ratios, during initiation of the structures, to high fluid fluxes along discrete conduits, as the structures propagate and develop large-scale permeability and penetrate hydrothermal reservoirs. At this second stage the discharging fluids were at high temperature and pressure and were reduced, owing to their transport upwards from deeper crustal levels; such fluids were predominantly of metamorphic origin, their characteristic high $\delta^{18}O$ reflecting equilibrium of the reservoir with crustal rocks at elevated temperatures in the source region.

Later in the tectonic evolution, as deeper crustal levels were exposed by erosion, such that conditions of lower ambient temperature and pressure pertained, an incursion of near-surface waters into faults occurred; these fluids were either formation brines in aquifers intersected by the fault or they were from direct downward penetration of surface fluids into the structures. Such fluids were oxidised and of lower $\delta^{18}O$, the former fact reflecting near-surface environments and the latter being commensurate with a component of meteoric continental surface water of lower $\delta^{18}O$ and/or metamorphic fluids of shallower level, where the $\delta^{18}O$ is buffered to smaller values by larger rock-water fractionations at the lower ambient temperatures. The high-temperature high ^{18}O and low-temperature fluid regimes of faults may proceed coevally, the former at deep crustal levels and the latter at shallow ones, juxtaposition

of the two taking place by subsequent vertical displacements on the structure. The flow of both deep-level (metamorphic) and shallow-level (meteoric) fluids has been implicated in contemporary seismic activity on the San Andreas fault by IRWIN and BARNES (1975) and SIBSON (1981, 1982), respectively.

At higher crustal levels a significant infiltration of meteoric water along major thrust faults has been identified. LEE et al. (1984) have shown that the δD and δ^{18}O and the apparent K-Ar ages of Mesozoic and Tertiary plutons in Nevada have been disturbed in proximity to the Snake Range décollement. In Oligocene plutons (37 Ma) deformed cataclastically, the δ^{18}O, the δD, and the K-Ar ages are as low as -2.5 per mil, -155 per mil, and 18 Ma respectively, owing to deformation combined with incursion of isotopically light thermal waters. For undeformed Jurassic plutons the δ^{18}O values are undisturbed, but both the δD and the K-Ar ages have been perturbed over distances of tens of metres below the décollement.

The Bitterroot Lobe, Sapphire Block detachment zone of western Montana is defined by a sequence of mylonitic granites 500 m thick, locally overprinted by chloritic breccias characterised by intense transgranular fracturing. KERRICH and HYNDMAN (1986) have shown that the ductile mylonites were formed at 550 ± 50 °C in the presence of magmatic or high-temperature metamorphic fluids. Chloritic breccias are depleted in ^{18}O by about 10 per mil relative to mylonitic precursors and appear to have formed under conditions of lower temperature (250 to 370 °C) and effective confining stress, acting as an aquifer for the infiltration of surface meteoric waters of low ^{18}O (δ^{18}O of -7 to -12 per mil).

At Lagoa Real, discharge of the fluids with low ^{18}O, of surface-water origin, probably took place at a depth of ≈ 15 km in the crust and at a relatively high temperature of $\approx$ 550 °C. This situation appears to have occurred during overriding of a sedimentary sequence with meteoric-water-recharged aquifers by high-grade gneisses during overthrusting. Thrusting of basement rocks over low-grade sediments is a typical feature of most mountain belts, and it has been suggested as an important component of Appalachian structure, as judged from high-resolution seismic profiling (COOK et al., 1980). Major fluid discharge must accompany such thrusting.

The role of metamorphic fluids in shear zones at deep crustal levels has been emphasised by BEACH and FYFE (1972), BEACH (1976), and KERRICH and FYFE (1981). ETHERIDGE et al. (1984) present evidence for high pore-fluid pressures during prograde regional metamorphism, with resultant low effective confining stress, leading to enhanced permeabilities and, in turn, to the local dominance of advective flow. All of these studies, including the present one, emphasise that large-scale fluid flow may occur at deep crustal levels under appropriate conditions. Recently this has received decisive corroboration in the encountering of high-temperature fluids at depths of ≈ 12 km in deep continental drilling. On the other hand, some shear zones appear to have been essentially chemically and hydrologically closed systems. This is the case in the Mieville shear zone transecting Hercynian granodiorite of the Aiguilles Ranges in Switzerland, where no significant excursions of δ^{18}O, oxidation state,

or composition occur from the protolith across the structure (KERRICH et al., 1980).

In addition to the mechanical effects of transient high fluid pressures in faults (KERRICH and ALLISON, 1978; SIBSON, 1981), a modification of ambient chemical conditions by fluids streaming through faults may play a role in silicate deformation. As discussed above, the oxidation state of iron in some structures indicates significant reduction by fluids, probably because of elevated partial pressures of hydrogen, and it is possible that such high P_{H_2} may influence the cracking behaviour of minerals in the fault zone. For instance, hydrogen embrittlement is a well-known phenomenon in metals and ceramics and is thought to be due to the chemisorption of hydrogen at fracture surfaces, which promotes nucleation of dislocations at crack tips (LYNCH, 1979; MICHALSKE and FREIMAN, 1982). HOBBS (1984) notes that, at an intracrystalline level, the incorporation of a hydrogen defect that is capable of acting as an acceptor in silicates leads to a strong dependence of point-defect chemistry on the fugacities of both water and oxygen.

Strontium isotope data have been employed in a number of studies of hydrothermal systems in an effort to address the solute source problem. Shear zones in the Willamaya Complex, Broken Hill, Australia, are plotted above the 1665 Ma isochron of the Potosi Gneiss host. ETHERIDGE and COOPER (1981) attribute the introduction of radiogenic strontium, coupled with SiO_2, K_2O, and Ba leaching, to large-scale fluid flow through the shear zone, where fluids ($^{87}Sr/^{86}Sr = 0.794$) had interacted with the Willamaya Complex metamorphics.

These, along with many other studies, demonstrate that where geological boundary conditions are appropriate, combined light-stable isotope and strontium isotope tracer studies may resolve the question of fluid and solute source reservoirs for domains of hydrothermally metasomatised faults.

Acknowledgments

Appreciation is expressed to C.-Y. Wang for the invitation to submit an article for the special issue of *The Journal of Pure and Applied Geophysics* on the internal structure of faults. D. Myers, D. S. Rogers, E. Van Hees, G. Nemcsok, S. Comline, and P. Bedard are thanked for permission to visit the Con, Dome, Aunor and Hollinger, Macassa, Darius, and Lamaque mines, respectively, and for supplying additional material. I am grateful to B. McLarty, L. M. Willmore, and J. Forth for analytical assistance. Mrs. G. McIntyre and Mrs. J. Miller are kindly thanked for conducting the typing and L. M. Willmore for drafting the diagrams. The Canadian Institute of Mining and Metallurgy is thanked for permission to reproduce some of the figures from Special Volume 27. I acknowledge with special gratitude numerous discussions with W. S. Fyfe and N. J. Price and the benefit of their incisive thoughts on 'fluids in the crust'. L. Lobato collected the rocks from Lagoa Real.

This research was supported by the National Research Council of Canada and

Ontario Geological Survey Research Funds. The light-stable isotope laboratory at the University of Western Ontario has been kept operational, thanks to the engineering skills of R. Jackman, R. Daddar, R. Kager, and R. Shirran.

REFERENCES

ALLISON, I. and KERRICH, R. (1979), 'History of deformation and fluid transport in shear zones at Yellowknife', in R. D. Morton (ed.). Proc. Gold Workshop, Yellowknife, N.W.T.

BARKER, F., 'Trondhjemites: Definition, environment and hypothesis of origin', in F. Barker (ed.), *Trodhjemites, Dacites, and Related Rocks.* Elsevier, New York, 1979.

BARKER, F., ARTH, J. G. and MILLARD, H. T., 'Archean trondhjemites of the southwestern Big Horn Mountains, Wyoming', in F. Barker (ed.), *Trondhjemites, Dacites, and Related Rocks.* Elsevier, Amsterdam, 1979, p. 401–414.

BEACH, A. (1976), *The interrelations of fluid transport, deformation, geochemistry and heat flow in early Proterozoic shear zones in the Lewissian complex.* Phil. Trans. Roy. Soc. London, Ser. A280, 569–604.

BEACH, A. and FYFE, W. S. (1972), *Fluid transport and shear zones at Scourie, Sutherland: Evidence for overthrusting?.* Contrib. Mineral. Petrol. *36*, 75–180.

BOYLE, R. W. (1961), *The geology, geochemistry, and origin of the gold deposits of the Yellowknife district.* Geol. Surv. Canada, Mem. *310*, 193.

BOYLE, R. W. (1977), *Discussion of: Iron reduction around gold-quartz veins, Yellowknife District, N.W.T.* Canada Econ. Geol.

BOYLE, R. W. (1979), *The geochemistry of gold and its deposits.* Geol. Surv. Canada Bull. *280*, 548 pp.

CLAYTON, R. N., O'NEIL, J. R. and MAYEDA, T. K. (1972), *Oxygen isotope exchange between quartz and water.* Geophys. Res. *77*, 3057—3067.

COLLERSON, K. D. and FRYER, B. J. (1978), *The role of fluids in the formation and subsequent development of early continental crust.* Contrib. Mineral. Petrol. *67*, 151–167.

COLVINE, A. C., ANDREWS, A. J., CHERRY, M. E., DUROCHER, M. E., FYON, A. J., LAVINGE, M. J., MACDONALD, A. J., MARMOT, S., POULSEN, K. H., SPRINGER, J. S. and TROOP, D. C. (1984), *An integrated model for the origin of Archean gold deposits.* Ontario Geol. Surv. Open File Rept. 5524, 98 p.

CONEY, P. J. (1980), *Cordilleran metamorphic core complexes: An overview.* Geol. Soc. Amer. Mem. *153*, 7–34.

COOK, F., BROWN, L. and OLIVER, J. (1980), *The Southern Appalachians and the growth of continents.* Sci. Am. *243*, 156–168.

CORDANI, U. G., DE (1982), *Interpretacao geocronologica de regiao de Lagoa Real, Ba.* Relatorio Integrado, unpublished ed.

CRITTENDEN, M. D., JR., CONEY, P. J. and DAVIS, G. H. (1980), *Cordilleran metamorphic core complexes.* Geol. Soc. Amer. Mem. *153*.

ETHERIDGE, M. A. and COOPER, J. A. (1981), *Rb/Sr isotopic and geochemical evolution of a recrystallized shear (mylonite) zone at Broken Hill.* Contrib. Mineral. Petrol. *78*, 74–84.

ETHERIDGE, M. A., COX, S. F., WALL, V. J. and VERNON, R. H. (1984), *High fluid pressures during regional metamorphism and deformation: Implications for mass transport and deformation mechanisms.* J. Geophys. Res. *89*, No. B6, 4344–4358.

FAURE, G., *Principles of Isotope Geology.* Wiley, Toronto, 1977, 464 p.

FITTON, J. G. (1985), *Basic volcanism associated with intraplate linear features.* Trans. Roy. Soc. London, Ser. A., in press.

FRANKLIN, J. M., ROSCOE, S. M., LOVERIDGE, W. D. and SANGSTER, D. F. (1983), *Lead isotope studies in Superior and Southern provinces.* Geol. Surv. Canada Bull. *351*, 60 p.

FRIEDMAN, I. and O'NEIL, J. R. (1977), 'Compilation of stable isotope fractionation factors of geochemical interest', in *Data of Geochemistry.* U.S. Geol. Surv. Prof. Paper 440.

FRYER, B. J., KERRICH, R., HUTCHINSON, R. W., PEIRCE, M. G. and ROGERS, D. S. (1979), *Archean precious metal hydrothermal systems, Dom Mine, Abitibi greenstone belt. I.* Canada J. Earth Sci. *16*, 421–439.

FYFE, W. S. and KERRICH, R. (1983), *Fluid release and mineralization associated with thrusting.* Fourth Int. Symp. Water-Rock Interaction, Misasa, Japan, Int. Assoc. Geochem. Cosmochem., 150–151.

FYFE, W. S. and KERRICH, R. (1985), *Fluids and thrusting.* Chem. Geology *49*, 353–362.

FYFE, W. S., PRICE, N. J. and THOMPSON, A. B., *Fluids in the Earth's Crust.* Elsevier, Amsterdam, 1978, 383 p.

FYON, J. A., SCHWARCZ, H. P. and CROCKET, J. H. (1984), *Carbonatization and gold mineralization in the Timmins area, Abitibi greenstone belt: Genetic links with Archean mantle CO_2-degassing and lower crust granulitization.* Geol. Assoc. Canada Prog. with Abstr. *9*, 65.

GATES, T. M. and HURLEY, P. M. (1973), *Evaluation of Rb–Sr dating methods applied to Matachewan, Abitibi, Mackenzie, and Sudbury dike swarms in Canada.* Canad. J. Earth Sci. *10*, 900–919.

GOLDING, S. D. and WILSON, A. F. (1983), *Geochemical and stable isotope studies of the No. 4 lode, Kalgoorlie, Western Australia.* Econ. Geol. *78*, 438–450.

GOODWIN, A. M. and RIDLER, R. H. (1970), *The Abitibi orogenic belt.* Canada Geol. Surv. Paper 70-40, 1–31.

GRESENS, R. L. (1967), *Composition – volume relations of metasomatism.* Chem. Geol. *2*, 47–65.

HART, S. R. and BROOKS, C. (1974), *Clinopyroxene-matrix partitioning of K, Rb, Cs, Sr, and Ba.* Geochim. Cosmochim. Acta *38*, 1799.

HOBBS, B. E. (1984), *Point defect chemistry of minerals under a hydrothermal environment.* J. Geophys. Res. *89*, No. B6, 4026–4038.

IRWIN, W. P. and BARNES, I. (1975), *Effects of geologic structure and metamorphic fluids on seismic behaviour of the San Andreas fault system in central and northern California.* Geology *4*, 713–716.

JAVOY, M. (1977), *Stable isotopes and geothermometry.* J. Geol. Soc. London *133*, 609–636.

JENSEN, L. S. (1976), *Regional stratigraphy and structure of the Timmins-Kirkland Lake area, District of Timiskaming, Ontario.* Dept. Mines Misc. Paper 67, 183 p.

JENSEN, L. S. (1978a), *Archean komatiitic, tholeiitic, calc-alkalic, and alkalic volcanic sequences in the Kirkland Lake area.* In Toronto '78 Field Trip Guidebook, Geol. Assoc. Canada, 237–259.

JENSEN, L. S. (1978b), *Larder Lake synoptic mapping project, District of Cochrane and Timiskaming.* Ont. Geol. Surv. Misc. Paper 94, 64–69.

JENSEN, L. S. (1980), *Gold mineralization in the Kirkland Lake–Larder Lake areas* Ont. Geol. Surv. Misc. Paper 97, 59–65.

JENSEN, L. S. and LANGFORD, F. F. (1983), *Geology and petrogenesis of the Archean Abitibi Belt in the Kirkland Lake area, Ontario.* Ont. Geol. Surv. Open File Rept. 5455, 520.

JOLLY, W. T. (1978), *Metamorphic history of the Archean Abitibi belt.* Geol. Surv. Canada, Paper 78–10, 367.

KENNEDY, L. P. (1985), *Geology and geochemistry of the Archean Flavarian Pluton, Noranda, Quebec, Canada.* Ph.D. thesis, University of Western Ontario, London, Ontario, Canada, 469.

KERRICH, R. (1983), *Geochemistry of gold deposits in the Abitibi greenstone belt.* CIM Special Paper 27.

KERRICH, R. (1985), *Archean lode gold deposits of Canada, Pt. I.* Proc. Symp. Archean Gold, Barberton, South Africa.

KERRICH, R. and ALLISON, I. (1978), *Vein geometry and hydrostatics during Yellowknife mineralization.* Canad. J. Earth Sci. *15*, 1653–1660.

KERRICH, R., ALLISON, I., BARNET, R. L., MOSS, S. and STARKEY, J. (1980), *Microstructural and chemical transformations accompanying deformation of granite in a shear zone at Mieville, Switzerland, with implications for stress corrosion cracking and superplastic flow.* Contrib. Mineral. Petrol. *73*, 221–242.

KERRICH, R. and FRYER, B. J. (1979), *Archean precious metal hydrothermal systems, Dome Mine, Abitibi greenstone belt: II. REE and oxygen isotope relations.* Canad. J. Earth Sci. *16*, 440–458.

KERRICH, R., FYFE, W. S. and ALLISON, I. (1977), *Iron reduction around gold-quartz veins, Yellowknife district, Northwest Territories, Canada.* Econ. Geol. *72*, 657–663.

KERRICH, R. and FYFE, W. S. (1981), *The gold-carbonate association: Source of CO_2, and CO_2 fixation reaction in Archaean lode deposits.* Chem. Geol. *33*, 265–294.

KERRICH, R. and FYFE, W. S. (1983), *The ^{18}O, temperature and ^{34}S of Archean ocean bottom water (2.8 Ga).* Geol. Surv. Canada Abstr., A37.

KERRICH, R. and HODDER, R. W. (1982), 'Archean lode gold and base metal deposits: Chemical evidence

for metal separation into independent hydrothermal systems', in R. W. Hodder and W. Petruk (eds.), CIM Spec. Vol. 24, Geology of Canadian Gold Deposits, 144–160.

KERRICH, R. and HYNDMAN, D. (1986), *Thermal and fluid regimes in the Bitterroot Lobe–Sapphire Block detachment zone: Evidence from $^{18}O/^{16}O$ and geologic relations.* Geol. Soc. Amer. Bull., *97*, 147–155.

KERRICH, R., KISHIDA, A. and WILLMORE, L. M. (1984), Geol. Assoc. Canada Prog. with Abstr. *9*, 78.

KERRICH, R., LOBATO, L., FYFE, W. S. and WILLMORE, L. M. (1986), *Shear zone hosted uranium deposits in overthrust Archean gneisses, Bahia, Brazil: Evidence on U provenance from Rb–Sr isotopic data.* Econ. Geol., in press.

KERRICH, R. and REHRIG, W. (1986) *Fluid motion associated with Tertiary mylonitization and detachment faulting: $^{18}O/^{16}O$ evidence from the Picacho metamorphic core complex.* G.S.A., in press.

KERRICH, R. and WATSON, G. P. (1984), *The Macassa Mine Archean lode gold deposit, Kirkland Lake, Ontario: Geology, patterns of alteration and hydrothermal regimes.* Econ. Geol. *79*, 1104–1130.

KING, R. W. (1983), *Auriferous 'Porphyry Zone', Taylor Township, Ontario: Petrology and geochemical relations.* B.Sc. thesis, University of Western Ontario, London, Ontario, Canada, 128.

KISHIDA, A. (1984), *Hydrothermal alteration zoning and gold concentration at the Kerr-Addison Mine, Ontario, Canada.* Ph.D. Thesis, Univ. Western Ontario, London, Canada, 231 p.

KISHIDA, A. and KERRICH, R. (1986), *Hydrothermal alteration zoning and gold concentration at the Kerr-Addison, Archean lode gold deposit, Kirkland Lake, Ontario.* Econ. Geol., in press.

KROGH, T. E., DAVIS, D. W., NUNES, P. D., and KORFU, F. (1982), *Archean evolution from precise U-Pb isotopic dating.* GAC/MAC Joint Annual Meeting, Winnipeg, Manitoba, Prog. with Abst. 7, 61.

KWONG, Y. T. J. and CROCKET, J. H. (1978), *Background and anomalous gold in rocks of an Archaean greenstone assemblage, Kakigi Lake area, Northwestern Ontario.* Econ. Geol. *73*, 50–63.

LA TOUR, T. E. (1981), *Significance of folds and mylonites at the Grenville Front in Ontario.* Geol. Soc. Amer. Bull. *92*, Pt. II, 997–1038.

LEE, D. E., FRIEDMAN, I. and GLEASON, J. D. (1984), *Modification of D values in eastern Nevada granitoid rocks spatially relatd to thrust faults.* Contrib. Mineral. Petrol. *88*, 288–298.

LOBATO, L. M., FORMAN, J. M. A., FUZIKAWA, K., FYFE, W. S. and KERRICH, R. (1983a), *Uranium in overthrust Archean basement, Bahia, Brazil.* Canad. Mineral. *21*, 647–654.

LOBATO, L. M., FORMAN, J. M. A., FYFE, W. S., KERRICH, R. and BARNETT, R. L. (1983b), *Uranium enrichment in Archean crustal basement associated with overthrusting.* Nature *303*, 235–237.

LOBATO, L. M., FUZIKAWA, K., FYFE, W. S. and KERRICH, R. (1983c), *Uranium enrichment in Archean basement: Logoa Real, Brazil.* Rev. Brasileira Geociencias *12*, 484–486.

LUDDEN, J. N., DAIGNEAULT, R., ROBERT, F. and TAYLOR, H. P. (1984), *Trace element mobility in alteration zones associated with Archean Au lode deposits.* Econ. Geol. *79*, 1131–1141.

LYNCH, S. P. (1979), *Mechanisms of hydrogen assisted cracking.* Metals Forum *2*, 189–200.

MCNEIL, A. M. and KERRICH, R. (1986), *Archean lamprophyric dykes gold mineralization, Matheson, Ontario: The conjunction of LIL-enriched mafic magmas, deep crustal structures and Au concentration.* Canad. J. Earth Sci., *23–3*, 324–343.

MICHALSEK, T. A. and FREIMAN, S. W. (1982), *A molecular interpretation of stress corrosion in silica.* Nature *295*, 511–512.

NESBITT, R. W. and SUN, S. S. (1976), *Geochemistry of Archean spinifex textured peridotites and magnesian tholeiites.* Earth Planet. Sci. Lett. *31*, 433–453.

NUNES, P. D. and JENSEN, L. S. (1980), *Geochronology of the Abitibi metavolcanic belt, Kirkland Lake area – progress report.* In E. G. Pye (ed.) Summary of Geochronology Studies 1977–1979, Ont. Geol. Surv. Misc. Paper 92, 40–45.

NUNES, P. D. and PYKE, D. R. (1980), *Geochronology of the Abitibi metavolcanic belt, Timmins – Matachewan area* – progress report. In E. G. Pye (ed.) Ont. Geol. Surv. Misc. Paper 92, 34–39.

OHMOTO, H. and RYE, R. O., *Isotopes of sulphur and carbon*, in H. L. Barnes (ed.), *Geochemistry of Hydrothermal Ore Deposits.* 2nd ed., Wiley, New York, 1979, 509–562.

O'NEIL, J. R. and TAYLOR, H. P. (1967), *The oxygen isotope and cation exchange chemistry of feldspars.* Am. Mineral. *52*, 1414–1437.

O'NEIL, J. R., CLAYTON, R. N. and MAYEDA, T. (1969), *Oxygen isotope fractionation in divalent metal carbonates.* Journ. Chem. Phys. *51*, 5547–5558.

PERCIVAL, J. A. and KROGH, T. E. (1983), *U–Pb zircon geochronology of the Kapuskasing structural zone and vicinity of the Chapleau-Foleyet area, Ontario.* Canad. J. Earth Sci. *20*, 830–843.

REHRIG, W. A. and KEITH, S. B. (1984), unpublished mapping.

ROBERT, F. and BROWN, A. C. (1984), *Chemical exchanges between gold mineralizing fluids and wall rocks at the Sigma Mine, Abitibi region, Quebec.* GAC-MAC Joint Ann. Meeting Progr. with Abstr. *9*, 100.

SIBSON, R. H., MOORE, J. MCM. and RANKIN, A. H. (1975), *Seismic pumping—A hydrothermal fluid transport mechanism.* J. Geol. Soc. London *131*, 653–659.

SIBSON, R. H. (1981), 'Fluid flow accompanying faulting: Field evidence and models', in D. W. Simpson and P. G. Richards (eds.), *Earthquake Prediction.* A.G.U. Maurice Ewing Series 4, 593–603.

SIBSON, R. H. (1982), Bull Seism. Soc. Am. *72*, 151–163.

STEIN, J. H., NETTO, A. M., DRUMMOND, D. and ANGEIRAS, A. G. (1980), *Nota preliminar sobre os processos de albitizacao uranifera de Lagoa Real (Bahia) e sua comparacao com os da URSS e Suecia.* Anais do 22nd Congr. Bras. Geol. Santa Catarina *3*, 1758–1775.

TAYLOR, H. P. (1974), *The application of oxygen and hydrogen isotope studies to problems of hydrothermal alteration and ore deposition.* Econ. Geol. *69*, 843–883.

TAYLOR, H. P., 'Oxygen and hydrogen isotope relations in hydrothermal mineral deposits', in H. L. Barnes (ed.), *Geochemistry of Hydrothermal Ore Deposits*, Wiley, New York, 1979, 236–277.

THOMSON, J. E. (1941a), *Geology of Gauthier Township, east Kirkland Lake area.* Ont. Dept. Mines Ann. Rept. *50*, Pt. 8.

VEIZER, J. and COMPSTON, W. (1974), $^{87}Sr/^{86}Sr$ *composition of seawater during the Phanerozoic.* Geochim. Cosmochim. Acta *38*, 1461–1484.

WANG, C.-Y. (1980), *Sediment subduction and frictional sliding in a subduction zone.* Geology *8*, 530–533.

WENNER, D. B. and TAYLOR, H. P. (1971), *Temperature of serpentinization of ultramafic rocks based on 0/0 fractionations between coexisting serpentine and magnetite.* Contrib. Mineral. Petrol. *32*, 165–185.

(Received 6th October 1985, revised 28th April 1986, accepted 30th April 1986)